

**Studies on the Regulation
of Expression of Iron-uptake-related Genes
in *Arabidopsis***

January 2014

Keita MATSUOKA

**Studies on the Regulation
of Expression of Iron-uptake-related Genes
in *Arabidopsis***

A Dissertation Submitted to
the Graduate School of Life and Environmental Sciences,
the University of Tsukuba
in Partial Fulfillment of the Requirements
for the Degree of Doctor of Philosophy in Science
(Doctoral Program in Integrative Environmental Sciences)

Keita MATSUOKA

Table of Contents

		Page
Abbreviations	-----	iii
Abstract	-----	1
Introduction	-----	5
Materials and Methods	-----	12
Plant material and growth conditions	-----	13
GA ₄ and PBZ treatment	-----	14
RNA extraction and cDNA synthesis	-----	14
quantitative RT-PCR analysis	-----	15
Semi-quantitative RT-PCR analysis	-----	16
Anatomical analysis	-----	17 エ
		ラ
		ー!
		ブッ
		クマ
		ーク
		が定
		義さ
		れて
		いま

Measurement of Fe content	-----	17
Plant transformation	-----	18
Histochemical analysis of GUS activity	-----	19
Results	-----	20
Part I: Effects of GA application on Fe-uptake-related genes in <i>Arabidopsis</i> root		
Effect of shoot-applied GA ₄ on <i>IRT1</i> and <i>FRO2</i> in <i>ga3ox1 ga3ox2</i>	-----	22
Fe content in root and shoot	-----	23
Effect of root-applied GA ₄ on <i>IRT1</i> and <i>FRO2</i> in <i>ga3ox1 ga3ox2</i>	-----	24
Part II: Fe-deficiency-induced responses in GA-deficient mutant		
Root hair formation under Fe-deficient conditions	-----	26
Fe-deficiency-induced expression of Fe-uptake-related genes	-----	26
The expression of GA biosynthesis genes in Fe-deficient condition	-----	27
Part III: Effect of GA on the regulation of <i>IRT1</i> expression		
Effect of GA ₄ application on bHLH-type TF genes in <i>ga3ox1 ga3ox2</i>	-----	31
under Fe-sufficient conditions		
FIT-independent GA effects on Fe-uptake-related genes under	-----	32
Fe-sufficient conditions		
FIT-dependent GA effects on Fe-uptake-related genes under	-----	34
Fe-deficient conditions		

Discussion	-----	36
Part I: Effect of applied-GA on Fe-uptake-related genes in	---	37
<i>Arabidopsis</i> root		
Part II: Fe-deficiency-induced response in GA-deficient mutant	---	41
Part III: Effect of GA on the regulation of <i>IRT1</i> expression	---	43
General Discussion	-----	48
References	-----	52
Table and Figures	-----	65
Acknowledgements	-----	93

Abbreviations

bHLH, basic Helix-Loop-Helix

Fe, Iron

FRO2, Ferric Reduction Oxidase 2

FIT, FER-like Iron Deficiency Induced Transcription Factor

GA, Gibberellin

GA2ox, GA 2-oxidase

GA3ox, GA 3-oxidase

GA20ox, GA 20-oxidase

GUS, β -glucuronidase

ICP-OES, Inductively coupled plasma - optical emission spectroscopy

IRT1, Iron-regulated Transporter 1

MS, Murashige and Skoog

PBZ, paclobutrazole

RT-PCR, Reverse transcription PCR

TF, Transcription factor

WT, wild-type

Abstract

In dicots, iron (Fe) is acquired from the soil by an iron transporter, *IRT1* and a Fe-reductase, *FRO2* localized at the root epidermis. The expression of *IRT1* and *FRO2* is induced by local and systemic signals under Fe-deficient conditions, however there is not known candidate signal transducer from shoots to roots. There are several reports about the effects of various phytohormones as a candidate of signal transducer (*e.g.* auxin, cytokinine and ethylene). Gibberellin (GA) is known as long-distance signal transducer, but the effects of GA on *IRT1* and *FRO2* expression have not been reported yet. The purpose of this study is to reveal the involvement of GA in the regulation of the expression of Fe-uptake-related genes in root.

In part I, GA₄ was applied to shoot of GA-deficient mutant, *ga3ox1 ga3ox2* which shows dwarf and dark-green leaves. After 3 days of GA₄ treatment, seedlings recovered to WT-like phenotype and the expression level of *IRT1* and *FRO2* increased in the higher concentration of GA₄ under Fe-sufficient conditions. In addition, Fe content in root of *ga3ox1 ga3ox2* was lower than in that of WT and enhanced by GA₄ application. On the other hand, GA₄ application to root did not increase in the expression of Fe-uptake-related genes. These results

show that aboveground-GA contributes to the promotion of the expression of Fe-uptake-related genes in root via other signal transducer and consequently absorption of Fe increased into root under Fe-sufficient conditions.

In part II, it was shown that GA was involved in the promotion of root hair formation under Fe-deficient conditions, but also the induction of Fe-uptake-related genes regardless of Fe conditions, however there was no change in the expression levels of GA-biosynthesis genes in shoot.

In part III, the effect of GA on the expression of bHLH-type TFs involved in *IRT1* regulation was investigated. Application of GA₄ to shoot also promoted the expression of *bHLH038* and *bHLH039*, as well as *IRT1*, but there was no significant change in *FIT* expression. Additionally, expression of *bHLH038* and *bHLH039*, except of *FIT* decreased in *ga3ox1 ga3ox2* compared with WT under Fe-sufficient conditions. *IRT1* expression also was induced by GA₄ application in not only Paclobutrazole (PBZ:an inhibitor for GA biosynthesis) -treated WT but also PBZ-treated FIT knockout mutant, *fit-2*. These data suggest that GA promoted the *IRT1*

expression via FIT-independent pathway under Fe-sufficient conditions. In contrast, all bHLH-type included in *FIT* TFs decreased in *ga3ox1 ga3ox2* compared with WT under Fe-deficient conditions. PBZ treatment suppressed *IRT1* expression in WT under Fe-deficient conditions, however there was no effect in *fit-2* mutant. Therefore, GA may involve in the positive regulation of *IRT1* via FIT-independent pathway under Fe-deficient conditions.

In conclusion, these data suggest the contribution of GA to the induction of Fe-uptake-related genes under Fe-sufficient and Fe-deficient conditions, possibly in FIT-independent and FIT-dependent manners, respectively.

Introduction

Iron (Fe) is an essential component for hemoglobin component in animals including human and so Fe deficiency causes common anemia, which is prevalent nutritional problem worldwide (Stoltzfus, 2001). Fe is also important for chlorophyll biosynthesis and several other processes such as respiration and enzymatic redox reaction in plants. When a plant is grown under Fe-limited conditions, chlorosis occurs in young leaves because the ring V formation in chlorophyll is catalyzed by CHL27, an Fe-dependent cyclase enzyme (Tottey et al., 2003). Under oxygen-rich and approximately neutral pH conditions, Fe mainly exists as the insoluble ferric form and plants are unable to obtain enough Fe from the soil. This ferric iron has an extremely low solubility in high-pH conditions. Thirty percentage of arable land of the world consists of alkaline soil, thus, Fe deficiency chlorosis of the crop is one of the agricultural problems. To overcome this problem, plants have several mechanisms. First, root hair formation is promoted under Fe-deficient condition (Romlied and Marschner, 1981; Mitchum et al., 2006), since the efficiency of Fe absorption is promoted by increase in root surface. Next, the excretion of proton H^+ or organic acids improves Fe solubility (Landsberg, 1981). Third, plants have developed

several Fe-uptake mechanisms categorized as strategy I (dicotyledons) and strategy II (monocotyledons) (Guerinot and Yi, 1994). For strategy II, mugineic acids (known as phytosiderophores) are secreted through TOM1 (transporter of mugineic acid 1), which is the efflux transporter of deoxymugineic acid, to the soil and chelate with ferric iron (Fe^{3+}) (Ma and Nonnoto, 1996; Nozoye et al., 2011). Fe^{3+} - mugineic acids complexes are absorbed into root cells through YELLOW-STRIPE1, an iron-phytosiderophore uptake transporter (Von Wiren et al., 1994; Curie et al., 2001). For strategy I, Fe^{3+} - chelate complexes are converted into Ferrous iron (Fe^{2+}) - chelate complexes by FERRIC REDUCTION OXIDASE 2 (FRO2) and Fe^{2+} is absorbed into root cells via IRON-REGULATED TRANSPORTER 1 (IRT1) (Robinson et al., 1999; Henriques et al., 2002). IRT1 and FRO2 are localized in root epidermal cells and the expression of *IRT1* and *FRO2* is strongly induced under Fe-limited conditions (Connolly et al., 2003; Vert et al., 2003). The transcription of these Fe-uptake-related genes is regulated by FER-LIKE IRON DEFICIENCY INDUCED TRANSCRIPTION FACTOR (FIT) (formerly described as bHLH029, FIT1, and FRU), which is a basic helix-loop-helix (bHLH) type transcription factor, under

Fe-deficient conditions (Bauer et al., 2007; Colangelo and Guerinot, 2004). However, over-expression of *FIT* alone is insufficient to induce the expression of *IRT1* and *FRO2* (Colangelo and Guerinot, 2004). Yuan et al. (2008) showed that FIT forms heterodimers with bHLH038 or bHLH039, and these complexes directly control the transcription of *IRT1* and *FRO2* by binding to the promoter of the genes.

On the contrary, high concentration of Fe causes toxicity to plants. Hydrogen peroxide (H_2O_2) is converted to the hydroxyl radical ($OH\cdot$) with Fe^{2+} and this reaction is well-known as Fenton reaction (Fenton, 1894). The $OH\cdot$ readily oxidizes DNA, protein and lipid in the intracellular component. Cleavage of DNA strand is caused by the oxidization of hydrogen atoms in the deoxyribose (Balasubramanian et al., 1998) and the oxidation product of nucleobases has ability to mispair during translesion synthesis (Consequences et al., 2002). DNA damage leads to mutation, or even worth, death. Therefore, plants must strictly regulate the amount of Fe absorption.

These Fe-uptake-related genes are regulated both by local induction within root tissue

and by long-distance signals from the shoot to roots (Vert et al., 2003). Fe deficiency is detected within the shoot and a signal is transmitted to roots to enhance the Fe-uptake mechanisms (Enomoto et al., 2007). In addition, *IRT1* and *FRO2* expression was repressed by foliar spray of Fe in Fe-sufficient plant, but did not in Fe-deficient plant (García et al., 2012). However, signal transduction pathways from the perception of Fe deficiency to *IRT1* and *FRO2* induction have not been identified for both local and long-distance regulation, and Fe-sensing mechanisms are still a matter of speculation (Vigani et al., 2013).

Several reports demonstrate the effect of various phytohormones on *IRT1* and *FRO2* expression. Auxin positively acts in *FRO2* induction under Fe-deficient conditions (Chen et al., 2010) and ethylene is also a positive regulator of *IRT1* and *FRO2* in *Arabidopsis* and cucumber (Lucena et al., 2006). In contrast, cytokinin and jasmonic acid repress the expression of *IRT1* and *FRO2* (Séguéla et al., 2008; Maurer et al., 2011). Treatment of brassinosteroid suppresses *CsIRT1* and *CsFRO1* expression in cucumber under Fe-deficient conditions (Wang et al., 2012).

The effect of gibberellin (GA) on *IRT1* and *FRO2* expression has not yet been

investigated. GA is a major phytohormone that promotes cell division and elongation, flowering, and germination (Hooley, 1994). Furthermore, GA is able to act as a long-distance signal transducer. For instance, GA derived from the upper shoot is involved in tissue reunion during wounding in cucumber hypocotyls (Asahina et al., 2002) and xylem expansion in *Arabidopsis* hypocotyls (Ragni et al., 2011). In addition, GA produced in the shoot promotes the expression of a xylem sap lectin (XSP30) in cucumber roots (Oda et al., 2003). Recently, stimulatory effect of GA on the Fe-uptake-related genes expression was shown in the result of microarray analysis. *IRT1* and *bHLH039* expression was increased more than 2-fold by the GA₄ application of shoot in the root of GA-deficient mutant, *ga3ox1 ga3ox2* (Bidadi et.al., *in press*).

In this study, I investigated the effect of GA on the expression of the Fe-uptake-related genes *IRT1*, *FRO2*, *FIT*, *bHLH038*, and *bHLH039* in *Arabidopsis*. Exogenous GA application promoted the expression of *IRT1* and *FRO2* mediated by bHLH038 and bHLH039 under Fe-sufficient conditions in *Arabidopsis*, possibly *via* the putative FIT-independent pathway; however, endogenous GA may be involved in the induction of *IRT1* and *FRO2* expression under

Fe-deficient conditions *via* the FIT-dependent pathway.

Materials and Methods

Plant material and growth conditions

Arabidopsis thaliana Columbia-0 (Col-0) ecotype was used as the WT. The *ga3ox1 ga3ox2* (*ga3ox1-3 ga3ox2-1*) GA-deficient mutant was provided by Riken institute (Mitchum et al., 2006). The *fit-2* mutant (SALK_126020, obtained from the Arabidopsis Biological Resource Center) and the homozygous genotype were verified by PCR using the primers listed in Table 1.

Seeds were surface-sterilized with sodium hypochlorite [1% (v/v) available chloride concentration] for 6 min, rinsed six times with distilled water, and kept in darkness at 4°C for two days. The *ga3ox1 ga3ox2* seeds were soaked in 100 μM GA₄ (Sigma) solution instead of water. The seeds were sown in MS medium (Murashige and Skoog, 1962) with 1.5% (w/v) agar and 0.5% (w/v) sucrose in square Petri dishes (140 mm \times 100 mm \times 14.5 mm; Eiken). For Fe-sufficiency or Fe-deficiency treatments, the seedlings were transplanted to either Fe-sufficient medium (100 μM Fe EDTA) or Fe-deficient medium [300 μM ferrozine (3-(2-pyridyl)-5,6-diphenyl-1,2,4-triazine -4',4''-disulfonic acid sodium salt; Sigma)]. Plates were incubated in continuous light at 22°C with a light intensity of 60 $\mu\text{mol m}^{-2} \text{s}^{-1}$.

GA₄ and PBZ treatment

For GA₄ treatment of shoots, 5 µL of 0, 0.01, 0.1, 1, or 10 µM GA₄ solution was applied to the shoot apex of 3-week-old seedlings (Bidadi et al., 2010). For GA₄ treatment of roots, 3-week-old seedlings were transplanted to medium supplemented with 0, 0.001, 0.01, 0.1, or 1 µM GA₄ for three days. The MS medium was supplemented with PBZ (Wako) dissolved in 0.1% (w/v) dimethylsulfoxide for a 1 µM PBZ final concentration. The optimal concentration of PBZ (1 µM) was determined by dose-response tests using both PBZ and GA₄ application to recover PBZ-induced effects on morphology.

RNA extraction and cDNA synthesis

Harvested samples were immediately frozen in liquid nitrogen. Total RNA was extracted using the RNeasy Mini Kit (Qiagen) following the manufacturer's protocol, and treated with DNase I Recombinant (Roche) to remove genomic DNA contamination. cDNA was

produced using the ReverTra Ace kit (Toyobo) with the oligo (dT) primer from 1 μg total RNA as a template. The 10- μL reaction solutions were diluted 15-fold with TE buffer.

Quantitative RT-PCR analysis

Transcript levels were quantitated using real-time RT-PCR with an Applied Biosystems 7300 system (Applied Biosystems). Amplification reactions were performed with 15 μL of reaction solution, containing with 7.5 μL GoTaq qPCR Master Mix (Promega), 0.15 μL of 100 \times Reference Dye, 3 μL of cDNA used as a template, and 0.2 μM of each primer described in Table 1. Primer dimer formation was monitored by control PCR reactions lacking template, and each PCR reaction was carried out in triplicate on one plate. Two-step PCR reactions were performed under the following conditions: 95 $^{\circ}\text{C}$ for 120 s; 40 cycles of 95 $^{\circ}\text{C}$ for 15 s and 60 $^{\circ}\text{C}$ for 60 s. The cycle threshold (Ct) values were determined using the ABI 7300 System Sequence Detection software (Applied Biosystems). The PCR efficiency (E) of each primer pair was deduced from the exponential phase of the amplification curves using the Liu & Saint-exp method with average

E values (Cikos et al., 2007). All amplification efficiencies were between 90 and 99%. Ct values were converted into relative quantities using the comparative Ct method, normalizing Ct values to *ACT7* as an internal control and incorporating the calculated PCR efficiency, with the following formula: Expression of target gene / Expression of *ACT7* = $(1+E)^{-Ct}$ target gene / $(1+E)^{-Ct}$ *ACT7* (Livak and Schmittgen, 2001; Aliparasti et al., 2012). Average values were calculated from three biological replicates.

Semi-quantitative RT-PCR analysis

Semi-quantitative RT-PCR was performed in 20 μ L of reaction solution that contained 2 μ L cDNA, TaKaRa Ex Taq (TaKaRa), and the primers described in Table 1. Three-step PCR was conducted: 94°C for 120 s; repeat cycles (22 and 25 cycles for *ACT7* and *FIT*, respectively) of 94°C for 30 s, 55°C for 30 s and 72°C for 60 s. The PCR products were detected by electrophoresis (20 min at 100 V) in 1.5% (w/v) agarose gels stained with ethidium bromide (Wako) and imaged with FAS-IV (Nippon Genetics).

Anatomical analysis

Root samples were obtained from 10-day-old seedlings and transplanted to either Fe-deficient or Fe-sufficient medium for 4 days. The root hairs on primary roots were observed using a stereomicroscope (MZFLIII, Leica). Root hair densities in every 1-mm segment up to 3 mm from the root tip were counted using ImageJ software (D. Abramoff et al., 2004).

Measurement of Fe content

WT and *ga3ox1 ga3ox2* plants were grown in medium containing 50 μ M Fe-EDTA. Solutions containing 0 or 10 μ M GA₄ were applied to the shoot apex every five days. Shoots and roots of 3-week-old seedlings were harvested and dried at 70°C for two days. Approximately 10 mg of each dried sample were digested in a mixture of 600 μ L hydrogen peroxide (30%; Wako) and 1,200 μ L nitric acid (60%; Wako) at 140°C for 4 h (Cheng et al., 2007). The digested samples were diluted with water and filtered using a 0.22- μ m filter (Millipore). Iron contents

were measured using ICP-OES (Perkin Elmer, Optima 7300DV) at the Chemical Analysis Center of the University of Tsukuba.

Plant transformation

An 1260 bp DNA fragment of the *bHLH038* genomic sequence upstream from initiation codon were amplified by PCR with iProof High-Fidelity DNA Polymerase (Bio-rad) and the primers (Reverse primer; 5'-TTTTTGCTTAATCAAGGACAAGG-3' and Forward primer; 5'-CACCTCCAGTTAAGACTAGAGTTAGTG-3). The PCR products were purified with Wizard SV Gel and PCR Clean-Up System (Promega) and cloned into the pENTR/D-TOPO entry vector (Invitrogen). These inserts were verified by sequencing using the M13 primers and then combined into pKGWFS7 destination vector with LR clonase II (Invitrogen). the recombinant plasmids was introduced into *Agrobacterium tumefaciens* GV3101 by the freeze-thaw method and transformed into *Arabidopsis ga3ox1 ga3ox2* mutant by floral dip method (Clough and Bent,

1998). T1 plants were selected for kanamycin resistance. Selected homozygous T3 or later progeny lines were used for further analysis.

Histochemical analysis of GUS activity

3-week-old seedlings grown in MS medium were treated with 10^{-5} M GA₄ on shoot or Fe-deficiency. After each treatments, histochemical detection of GUS activity was performed with 5-bromo-4-chloro-3-indolyl-b-glucuronide (X-Gluc) as a substrate. Whole plants were immersed in X-Gluc solution (0.1 M X-Gluc, 0.1 M NaPO₄ pH 7.0, 10.0 mM EDTA, 0.1% Triton X-100, 1.0 mM K₃Fe(CN)₆, 20% MeOH), subjected to a vacuum for 5 min and incubated at 37°C. Stained samples were transferred to 100% EtOH to stop the reaction.

Results

Part I:

**Effects of GA application on Fe-uptake-related genes
in *Arabidopsis* root**

Effect of shoot-applied GA₄ on *IRT1* and *FRO2* in *ga3ox1 ga3ox2*

Arabidopsis ga3ox1 ga3ox2 double mutant was used as a GA-deficient mutant.

Gibberellin 3-oxidase (GA3ox) converts bio-inactive GA₉ to bioactive GA₄ at the final step in the GA biosynthesis pathway (Yamaguchi et al., 1998). In *Arabidopsis*, the GA3ox gene family consists of four members, At1g15550 (*GA3ox1/GA4*), At1g80340 (*GA3ox2*), At4g21690 (*GA3ox3*), and At1g80330 (*GA3ox4*). *GA3ox3* and *GA3ox4* are mainly expressed in reproductive organs and the amount of bioactive GA₄ is significantly decreased in vegetative organs of a *GA3ox1* and *GA3ox2* double knockout line (Mitchum et al., 2006). Therefore *ga3ox1 ga3ox2* mutant showed a dwarf phenotype and were used as GA-deficit mutant.

Seedlings of *ga3ox1 ga3ox2* were stunted and had dark-green leaves (Fig. 1A; 0 M GA₄). Application of GA₄ on the shoot apex of 3-week-old *ga3ox1 ga3ox2* plants promoted shoot growth and recovered normal leaf color, in contrast to the mock treatment (Fig. 1A, B), confirming that the exogenous GA₄ treatment partially recovered the phenotype of the mutant, which is derived from GA deficiency. Real-time reverse transcription-PCR (RT-PCR) showed

that the *IRT1* and *FRO2* expression levels were increased 2- and 3-fold by the application of 1 or 10 μ M GA₄ onto the shoot apex, respectively (Fig. 1C).

Fe content in root and shoot

Because shoot-applied GA₄ enhanced the expression of Fe-uptake-related genes, Fe concentrations on shoot and root were investigated in *ga3ox1 ga3ox2* mutants with or without GA₄ application, as compared with WT. Fe concentration and total content in *ga3ox1 ga3ox2* roots increased about 1.4- and 1.6-fold by GA₄ treatment compared to the mock treatment, respectively (Fig. 2A, B). However, the shoot Fe concentration per gram dry weight in *ga3ox1 ga3ox2* increased 1.7-fold over that of WT; GA₄ application reduced the Fe content to the level in the WT (Fig. 2C) and there was no difference in the total Fe content per shoot (Fig. 2D). These results may be caused by the promotion of shoot growth from GA₄ application along with the promotion of Fe uptake into root, and the recovery from high Fe-content in *ga3ox1 ga3ox2* shoots.

Effect of root-applied GA₄ on *IRT1* and *FRO2* in *ga3ox1 ga3ox2*

To determine if the shoot-applied GA₄ effect in *ga3ox1 ga3ox2* was due to GA₄ itself or other factors converted from or triggered by GA₄ within the shoot, roots were grown in MS medium containing GA₄. Shoot growth was increased 3 days after GA₄ treatment of roots (Fig. 3A, B). At that time the roots were harvested and Fe-uptake-related gene expression was examined. Unlike shoot-applied GA₄ treatment, root-applied GA₄ treatment did not substantially increase *IRT1* and *FRO2* expression (Fig. 3C), suggesting that GA₄ may not be autonomous in the root and may require shoot functions as well.

Part II:

Fe-deficiency-induced responses in GA-deficient mutant

Root hair formation under Fe-deficient conditions

The morphological phenotypes in WT and the *ga3ox1 ga3ox2* GA-deficient mutant were compared under Fe-limited conditions to determine if GA is involved in the Fe-deficiency response in *Arabidopsis*. Fe deficiency induces root-hair formation and growth (Romlied and Marschner, 1981; Mitchum et al., 2006). The increase in root surface area enables the highly efficient acquisition of nutrients such as Fe. Root-hair density increased with Fe deficiency in WT and to a lesser extent in *ga3ox1 ga3ox2*, particularly in the 1- to 2-mm segment from the root tip (Fig. 4A, B). These results suggest that GA is involved in root-hair formation under Fe-deficient conditions.

Fe-deficiency-induced expression of Fe-uptake-related genes

Under Fe-deficient conditions, the expression of Fe-uptake-related genes, such as *IRT1* and *FRO2* strongly increased in both WT and *ga3ox1 ga3ox2*, but the induction of genes in *ga3ox1 ga3ox2* was about half the level of that in WT (Fig. 5A). Additionally, the suppression of

IRT1, as well as the morphology of shoots (Fig. 5C), was slightly recovered by GA₄ treatment of shoots in *ga3ox1 ga3ox2* (Fig. 5B). The expression levels of *IRT1* significantly decreased in *ga3ox1 ga3ox2*, even under Fe-sufficient conditions. These results suggest that the synthesis of bioactive GA may be involved in the induction of Fe-uptake-related genes, especially under Fe-deficient conditions.

The expression of GA biosynthesis genes in Fe-deficient conditions

Because GA contributed to the induction of Fe-uptake-related genes under Fe-deficient conditions (Fig. 5A), I examined whether Fe deficiency causes changes in the levels of bioactive GA by affecting the expression of GA biosynthetic and catabolic genes. GA20ox catalyzes three oxidation steps from GA₁₂ and GA₅ to GA₉ and GA₂₀, respectively (Olszewski et al., 2002). Therefore, this enzyme produces the precursor of bioactive GAs. GA20ox is considered a rate-limiting enzyme during the GA biosynthetic pathway because *GA20ox*-overexpressing transformants have been shown to have long stems and hypocotyls (Huang et al., 1998; Coles et

al., 1999). In contrast, the suppression of *GA20ox* or *ga20ox1 ga20ox2 ga20ox3* mutant results in dwarf phenotypes (Coles et al., 1999; Rieu et al., 2008b; Plackett et al., 2012). In Fig. 6A-D, the gene expression levels are shown as values relative to those of *ACT7*. In shoots, *GA20ox3* was only significantly reduced under Fe-deficient conditions, but *ga20ox3* showed an extremely low expression level compared with other *GA20ox* genes and there were no significant differences in the expression levels of other *GA20ox* or *GA3ox* genes (Fig. 6A), therefore total expression levels of *GA20ox* as well as *GA3ox* genes were constant. In contrast, *GA2ox* promotes the inactivation of bioactive GAs and is important for the regulation of bioactive GA levels (Curtis et al., 2005; Rieu et al., 2008a), and it is known that *GA2ox1* and *GA2ox2* among six *GA2ox* genes (*GA2ox1* to *GA2ox8*, except for *GA2ox5*) were promoted by phosphate starvation (Jiang et al., 2007). The levels of *GA2ox* genes in shoots also did not change under Fe-deficient conditions (Fig. 6B). These results suggest that the levels of bioactive GAs in shoots remain nearly constant during Fe deficiency.

In roots, the expression levels of *GA3ox1* was slightly decreased (Fig. 6C) and the levels

of *GA2ox* genes increased significantly under Fe-deficient conditions (Fig. 6D), suggesting that the levels of bioactive GA decreased under Fe-deficient conditions. Thus, the alteration of bioactive GA levels in response to Fe deficiency was different between shoots and roots, and there appeared to be no correlation between the bioactive GA levels and the expression of Fe-uptake-related genes under Fe-deficient conditions.

Part III:

Effect of GA on the regulation of *IRT1* expression

Effect of GA₄ application on bHLH-type TF genes in *ga3ox1 ga3ox2* under

Fe-sufficient conditions

The gene expression of bHLH-type TF involved in the *IRT1* induction was investigated to reveal the mechanism of regulation of *IRT1* expression. One and 10 μM GA₄ applications on shoot up-regulated *IRT1* expression in *ga3ox1 ga3ox2* (Fig. 1C). *bHLH039* expression was induced at all GA₄ concentrations (Fig. 7A). Specifically, *bHLH038* was extremely induced ~5- and ~8-fold by the 1 and 10 μM GA₄ treatments, respectively, and had a strong relationship with *IRT1/FRO2* expression. In contrast, *FIT* expression did not increase with GA₄ application (Fig. 7A). To reveal the relationship between *IRT1* and bHLH-type TF, these gene expression patterns were compared in time course after GA₄ application on shoot of *ga3ox1 ga3ox2*. *IRT1* and *bHLH038* expression increased after 48 and 24 hours of GA₄ treatment, respectively, however *FIT* expression decreased after 6 hours of treatment (Fig. 8). Thus, GA₄ application induced *bHLH038* expression earlier than *IRT1* expression. In contrast, there was no difference for *IRT1* expression by GA₄ applications on root in *ga3ox1 ga3ox2* (Fig. 3C). The expression of *FIT*

decreased at all GA₄ concentrations, and the expression of *bHLH038* and *bHLH039* increased only slightly (Fig. 7B).

The levels of *bHLH038* and *bHLH039*, which are induced in shoots under Fe-deficient conditions (Wang et al., 2007), also increased in shoots following GA application onto the shoot (Fig. 9A). *bHLH038* promoter was introduced in upstream of GUS. *pbHLH038::GUS* was transformed to *ga3ox1 ga3ox2*. Strong GUS staining was exhibited in both shoot and root by GA₄ application on shoot, although the GUS staining was already shown in lateral root of mock treatment (Fig. 9B).

FIT-independent GA effects on Fe-uptake-related genes under

Fe-sufficient conditions

In order to investigate effect of endogenous GA on bHLH-type TFs, these expressions were compared between WT and *ga3ox1 ga3ox2*. *bHLH038* and *bHLH039* expression, as well as *IRT1*, decreased in *ga3ox1 ga3ox2* compared with WT under Fe-sufficient conditions (Fig. 5A,

10A), on the other hand, expression level of *FIT* was similar in WT and *ga3ox1 ga3ox2* under Fe -sufficient conditions (Fig. 10A). FIT binds to the promoter regions of *IRT1* and *FRO2*, forming a heterodimer with bHLH038 or bHLH039, and directly regulates the induction of these genes under Fe-deficient conditions (Yuan et al., 2008). To examine whether FIT is necessary for the GA₄-induced gene expression, GA₄ was applied to a loss-of-function *FIT* mutant, in which neither FIT mRNA nor protein was detected: a *fit-2* mutant containing a T-DNA insert within the third exon of the gene (Sivitz et al., 2011). After germination, WT and *fit-2* were grown in MS medium supplemented with paclobutrazol (PBZ), an inhibitor of GA biosynthesis, to reduce the endogenous GA levels (Antonio et al., 2005). PBZ-treated dwarf seedlings were applied with GA₄ on shoot and recovered the leaf color and leaf size after three days. According to quantitative RT-PCR analysis, the products of *FIT* amplified from upstream of the T-DNA insertion position were slightly detected in *fit-2* (Fig. 11A). However, no RT-PCR products covering the region spanning the T-DNA were amplified from *fit-2* (Fig. 11B). Because the *fit-2* mutant has previously been used as a FIT-deficient mutant in several studies (Colangelo and

Guerinot, 2004; Sivitz et al., 2011; Hong et al., 2013), the *fit-2* mutant was assumed to be a knockout line. *IRT1* and *FRO2* expression in *fit-2* was substantially weaker than in WT, but the expression of both was upregulated by applications of GA₄ (Fig. 11). In *fit-2*, *bHLH038* and *bHLH039* expression was higher than in WT, and shoot-applied GA₄ upregulated the expression of these genes (Fig. 11). In contrast, *FIT* expression was decreased by GA₄ treatment of the WT (Fig. 11).

FIT-dependent GA effects on Fe-uptake-related genes under Fe-deficient conditions

IRT1 expression decreased in *ga3ox1 ga3ox2* under both Fe-sufficient and deficient conditions (Fig. 5A). In contrast to the Fe-sufficient conditions, all bHLH-type TF genes including *FIT* showed lower expression levels in *ga3ox1 ga3ox2* under Fe-deficient conditions (Fig. 10A). To reveal this decreased expression of *IRT1* is due to lower *FIT* expression, GA-biosynthesis inhibitor PBZ was applied to WT and *fit-2* mutant. *IRT1* expression was

suppressed by PBZ treatment in WT under Fe-deficient conditions, however, there were no effect for *IRT1* in *fit-2* (Fig. 12).

Discussion

Part I: Effects of GA application on Fe-uptake-related genes in *Arabidopsis* root

GA₄ application up-regulated the expression of *IRT1* in shoot of *ga3ox1 ga3ox2*, therefore it was expected that the endogenous GA regulated the Fe-uptake-related genes.

Tanimoto (1987) suggested that endogenous GA is sufficient under ‘normal’ root growth conditions, and the role of GA can be examined through loss-of-function analyses using mutants lacking GA biosynthetic genes or in seedlings treated with a GA-biosynthesis inhibitor such as PBZ or uniconazole. Therefore, I showed that *IRT1* and *FRO2* were upregulated by GA₄ application to *ga3ox1 ga3ox2* shoots (Fig. 1C). Application of 1 and 10 μM GA₄ was sufficient to promote shoot growth (Fig. 1A, B) and the expression of *IRT1* and *FRO2* in roots (Fig. 1C).

Exogenous radioactive-labeled GA is mobile in plant tissues (Proebsting et al., 1992). In *Arabidopsis*, radioactive-labeled GA₄ can be detected in the shoot apex after application to leaves (Eriksson et al., 2006), indicating that exogenously-applied GA₄ can be transported between organs. However, direct GA₄ application to roots only slightly induced the expression of *IRT1* and *FRO2* (Fig. 3C). These results indicate that GA₄ mainly acts as a trigger in the shoots

for the induction of these genes in roots and suggests that shoot-applied GA₄ may activate a signal transducer that is transported to roots. For instance, it has been proposed that micro-RNAs (miRs) were one of the candidate signal transducers from shoots to roots for inducing Fe-uptake-related genes in roots. Kong and Yang (2010) proposed that any miR may be likely involved in the Fe deficiency response as well as miR399 and miR395 in phosphate and sulfate deficiency, respectively (Pant et al., 2008; Liang et al., 2010). However, among a few GA-responsive miRs previously reported (Achard et al., 2004; Liu et al., 2009), there was no overlap with the Fe-responsive miRs. Further studies using transcriptomic or metabolomic approaches will be needed to identify the signal transducer, such as auxin, because auxin is transported from shoot to root and indicate cross-talk with GA.

I showed that the application of exogenous GA₄ to shoots upregulated the expression of *IRT1* and *FRO2*, and the *IRT1* expression (except for *FRO2*) decreased in the GA-deficient mutant under Fe-sufficient conditions (Fig. 5A). There have been no reports that the expression of *IRT1* and *FRO2* is altered in phytohormone-deficient mutants under Fe-sufficient conditions,

although exogenously applied phytohormone has been shown to influence the expression of those genes in other studies (Séguéla et al., 2008, Chen et al., 2010, Maurer et al., 2011). Therefore, this is the first report showing the possible involvement of endogenous hormones in the regulation of *IRT1* under Fe-sufficient conditions.

Because *IRT1* and *FRO2* are localized in root epidermal cells and absorb Fe from the rhizosphere (Vert et al., 2003), I tested whether GA_4 application elevated the Fe content in shoots and roots. The accumulation of Fe in *ga3ox1 ga3ox2* roots was promoted by shoot-applied GA_4 (Fig. 2A). In contrast, the Fe concentration in *ga3ox1 ga3ox2* shoots was similar to the level in the WT, although the Fe content per shoot was not altered by shoot-applied GA_4 (Fig. 2C, D). This suggests that GA_4 application may not have promoted Fe translocation from the roots to the shoot, and thus the regulation of long-distance Fe transport may not be controlled by GA. Iron translocation mechanisms may be suppressed in order to maintain Fe homeostasis and prevent the accumulation of high levels of Fe in the shoots of the *ga3ox1 ga3ox2* GA-deficient dwarf mutants. Since GA-deficient mutants typically have dark-green leaves with elevated chlorophyll

content (Peng and Harberd, 1997); GA indirectly promotes chloroplast division through the effect of leaf mesophyll cell expansion (Jiang et al., 2012), it seems that dark-green leaves and high Fe concentrations might be the result of small cell size in GA-deficient mutants.

Several reports have shown the effect of root GA on Fe homeostasis in plants.

Application of uniconazole to roots has been shown to have no effect on shoot Fe concentrations in cucumber (Sekimoto et al., 1998). In rice, PBZ treatment decreased the root Fe concentration but had no effect on shoots (Pan et al., 1991). Treatment of roots with GA₃ promoted root Fe absorption and transport to above-ground tissues in marrow bean (Kannan and Mathew, 1970).

Our results are consistent with those of these reports that showed no consistent effects of GA application on Fe homeostasis. This may be due to the various experimental conditions with different plant species.

Part II: Fe-deficiency-induced response in GA-deficient mutant

The up-regulation of *IRT1* and *FRO2* by shoot-applied GA₄ suggests that GA may induce a signaling factor for Fe homeostasis. *IRT1* expression is thought to be induced by Fe deficiency in shoots (Vert et al., 2003), because it is suppressed by removing leaves (Enomoto et al., 2007) and is consistently up-regulated in the *FRD3* (*man1*) mutant, which has deficient Fe transport from the roots to the shoot resulting in high root Fe concentration (Delhaize, 1996; Durrett et al., 2007). Root-hair formation is suppressed under Fe-deficient conditions in *ga3ox1 ga3ox2* compared with WT (Fig. 4B). The *gal-3* GA-deficient mutant also has shorter root hairs when grown in low phosphate (Jiang et al., 2007). Thus, GA-mediated root-hair formation is not related to the perception of Fe concentration in shoots. In contrast, the expression pattern of Fe-uptake-related genes was similar between *ga3ox1 ga3ox2* and WT under Fe-deficient conditions (Fig. 5A), suggesting that root-hair formation and the induction of Fe-uptake-related genes have different mechanisms during Fe deficiency. These results indicate that the effect of the absence of bioactive GA is not as significant and is perhaps masked by the

response induced by Fe deficiency. In addition, endogenous GA level in shoot decreased under Fe-deficient condition (Fig. 6). Sekimoto et al. (2002) reported that Fe deficiency reduced GA content but had no effect on Fe concentration in shoots. The decrease of GA may be adaptation of environmental stress by growth suppression. PBZ treatment did not alter foliar Fe concentration in low Fe conditions (Sankhla et al., 1986). Thus, GA may not contribute to Fe uptake and transport under Fe-deficient conditions. On the other hand, *IRT1* and *FRO2* expression decreased in *ga3ox1 ga3ox2* under Fe-sufficient conditions (Fig. 5A). GA may work for the expression of Fe-uptake-related genes under Fe-sufficient conditions.

Part III: Effect of GA on the regulation of *IRT1* expression

I evaluated bHLH-type transcription factors such as FIT, bHLH038, and bHLH039 to determine how GA regulates the expression of *IRT1* and *FRO2* in roots. Application of GA₄ promoted the expression of *bHLH038* and *bHLH039*, except for *FIT* (Fig. 7A, 8). Additionally, in the *fit-2* mutant, the expression of *IRT1* and *FRO2* was enhanced by shoot-applied GA₄; however, the expression level of *IRT1* and *FRO2* in *fit-2* was substantially reduced compared to the WT (Fig. 11). Induction of *bHLH038* occurred earlier than that of *IRT1* by GA₄ application (Fig. 8). These results suggest that factors other than the known FIT/bHLH038 (or bHLH039) heterodimer may regulate *IRT1* and *FRO2* expression. According to calculation of multiple sequence alignment from BLAST search against TAIR10 database, FIT showed lower homology to AMS/bHLH021, bHLH027 and bHLH035 (22, 18, and 20% identity, respectively) (Fig. 13A, B), which were known to have different functions from Fe-uptake (Thorstensen et al., 2008; Jin et al., 2011). Therefore, FIT homologues gene instead of FIT may not play a role in *IRT1* regulation. On the other hand, because bHLH038 and bHLH039 present as tandem gene

duplication in the genome and show functional redundancy to bHLH100 and bHLH101, has very high homology (Fig. 13A, B) (Wang et al., 2007; Wang et al., 2012b), analysis of bHLH038 and bHLH039 have hardly progress about *IRT1* regulation. Auxin acts as an inducer of *FRO2* via FIT-mediated regulation under Fe-deficient conditions (Chen et al., 2010), whereas the suppression of *IRT1* and *FRO2* by cytokinin and jasmonic acid is independent of FIT (Séguéla et al., 2008; Maurer et al., 2011). Thus, the GA-mediated induction of *IRT1* and *FRO2* shown here may share the signaling pathway used for cytokinin and jasmonic acid.

With the exception of *FIT*, the bHLH transcription factor genes such as *bHLH038* and *bHLH039*, especially *bHLH038*, showed expression patterns similar to those of *IRT1* and *FRO2* (Fig. 1C, 5A, 7A, 8, 10A). The expression of *bHLH038* was particularly sensitive to GA application and deficiency and the expression was enhanced by GA application (even in *fit-2*) under Fe-sufficient conditions (Fig. 11). Since the expression of *bHLH038* and *bHLH039* increased in Fe-uptake-deficit mutants such as *fit* (Wang et al., 2007), feedback regulation may control their expression. Moreover, it was reported that bHLH038 alone could not upregulate

IRT1 and *FRO2* expression (Yuan et al., 2008). Therefore, I supposed that bHLH038 and bHLH039 form heterodimers with other bHLH-type transcription factors or with *FIT*, accompanied by some accessory proteins to control the expression of *IRT1* and *FRO2*.

Here, I am the first to suggest that GA application may positively control *IRT1* expression *via* a putative FIT-independent pathway. There have been reports that *IRT1* is negatively controlled by other phytohormones *via* a FIT-independent pathway (Séguéla et al., 2008; Maurer et al., 2011). In contrast, the expression of *IRT1*, *FRO2*, and *FIT* decreased significantly in *ga3ox1 ga3ox2* under Fe-deficient conditions (Fig. 5A, 10A) and *IRT1* expression in *fit-2* was not suppressed by PBZ treatment (Fig. 12). Therefore, FIT may be involved in the suppression of *IRT1* in GA-deficient plants.

The effect of GA on *IRT1* expression may have the different mechanism depending on the Fe conditions, but GA was found to positively regulate the *IRT1* expression either in Fe sufficient or deficient condition. Therefore, *IRT1* expression in root may be induced by multiple long-distance signals from shoot. Some of previous reports suggested that *IRT1* expression in

root might be induced by multiple long-distance signals from shoot (Enomoto et al., 2007; Chen et al., 2010). Since auxin acts upstream of *IRT1* and *FIT* (Chen et al., 2010; Bacaicoa et al., 2011) and exhibits cross-talk with GA (Willige et al. 2011; 2012), transport of auxin from shoot to root may be involved in the regulation of *IRT1* expression by GA. On the other hand, Enomoto et al. (2007) showed through leaf-excision experiments that *NtIRT1* expression is positively correlated with leaf size in tobacco. Therefore, shoot-growth including leaf development and chloroplast division controlled by GA (Achard et al., 2009; Jiang et al., 2012) may be involved in the regulation of *IRT1* expression by GA. Since Fe in shoot is essential for rapid growth and various metabolic processes including photosynthesis and respiration and its concentration in shoot is tightly regulated by *IRT1* expression in response to Fe conditions (Baxter et al., 2008), the metabolic changes caused by GA in shoot may contribute to control of *IRT1* expression in root.

In conclusion, my work suggests that GA may be involved in the regulation of the expression of Fe-uptake-related genes *via* putative FIT-independent pathways under Fe-sufficient

conditions and *via* FIT-dependent pathways under Fe-deficient conditions.

General Discussion

To date, various phytohormones have been reported to regulate the *IRT1/FRO2* expression. Auxin and ethylene promote these expression whereas cytokinin, brassinosteroid, abscisic acid jasmonic acid and salicylic acid repress the expression (Lucena et al., 2006; Séguéla et al., 2008; Dellagi et al., 2009; Chen et al., 2010; Pe et al., 2010; Maurer et al., 2011; Wang et al., 2012a). GA had been only the unrevealed phytohormone for the effect on *IRT1/FRO2* expression. Here, I demonstrated that GA positively regulates the *IRT1/FRO2* expression. Effect of GA is well-known as the promotion of cell division and cell expansion (Hooley, 1994). Therefore, GA-deficient mutants exhibit the dwarf phenotype and restore the WT phenotype by GA application (Mitchum et al., 2006). Interestingly, the following two hypotheses about interaction between the plant growth and *IRT1/FRO2* expression have been proposed. i) Root growth dependent regulation (Séguéla et al., 2008). ii) Shoot size dependent regulation (Enomoto et al., 2007). GA promotes both root and shoot growth. Therefore, these hypotheses are consistent with the effect of GA on *IRT1/FRO2* expression, however, *IRT1/FRO2* expression was not altered

despite the promotion of root growth by GA₄ application to root. Therefore, this result supports the latter hypothesis.

Existence of FIT-independent pathway previously reported in inhibitory by effects of cytokinin and jasmonic acid (Séguéla et al., 2008; Maurer et al., 2011), however, GA showed positive effect on *IRT1/FRO2* unlike cytokinin and jasmonic acid. This provides evidence for the presence of FIT-independent pathway. On the other hand, auxin and ethylene induce *IRT1/FRO2* expression via FIT-dependent pathway (Chen et al., 2010; Lingam et al., 2011). Therefore, it is possible that effect of GA involve the crosstalk between other phytohormones on the regulation of *IRT1/FRO2* expression. Microarray analysis was performed to identify root-expressed genes that was responded by GA on shoot (Bidadi et.al., *in press*). The expression of some auxin-response or ethylene-biosynthesis genes was increased by GA application, suggesting that GA may promote the auxin and ethylene levels on root. In contrast, the response genes of ABA, known to show an antagonistic effect against GA were not found in microarray data. In order to reveal the regulation of *IRT1/FRO2* expression, it would be necessary to understand the

interaction between phytohormones.

References

Achard P, Gusti A, Cheminant S, Alioua M, Dhondt S, Coppens F, Beemster GTS, Genschik P

(2009) Gibberellin signaling controls cell proliferation rate in Arabidopsis. *Curr Biol* **19**: 1188–1193

Achard P, Herr A, Baulcombe DC, Harberd NP (2004) Modulation of floral development by a

gibberellin-regulated microRNA. *Development* **131**: 3357–3365

Aliparasti MR, Alipour MR, Almasi S, Feizi H (2012) Effect of ghrelin on aldolase gene expression in

the heart of chronic hypoxic rat. *Int J Endocrinol Metab* **10**: 553–557

Antonio J, Grossi S, Moraes PJ De, Tinoco SDA, Barbosa JG, Finger FL, Cecon PR (2005) Effects

of paclobutrazol on growth and fruiting characteristics of “Pitanga” ornamental pepper. *Acta Hort*

683: 333–336

Asahina M, Iwai H, Kikuchi A, Yamaguchi S, Kamiya Y, Kamada H, Satoh S (2002) Gibberellin

produced in the cotyledon is required for cell division during tissue reunion in the cortex of cut

cucumber and tomato hypocotyls. *Plant Physiol* **129**: 201–210

Bacaicoa E, Mora V, Zamarreño AM, Fuentes M, Casanova E, García-Mina JM (2011) Auxin: a

major player in the shoot-to-root regulation of root Fe-stress physiological responses to Fe

deficiency in cucumber plants. *Plant Physiol Bioch* **49**: 545–556

Balasubramanian B, Pogozelski WK, Tullius TD (1998) DNA strand breaking by the hydroxyl radical

is governed by the accessible surface areas of the hydrogen atoms of the DNA backbone. *Proc Natl*

Acad Sci USA **95**: 9738–43

Bauer P, Ling H-Q, Guerinot M Lou (2007) FIT, the FER-LIKE IRON DEFICIENCY INDUCED TRANSCRIPTION FACTOR in Arabidopsis. *Plant Physiol Bioch* **45**: 260–261

Baxter IR, Vitek O, Lahner B, Muthukumar B, Borghi M, Morrissey J, Guerinot M Lou, Salt DE (2008) The leaf ionome as a multivariable system to detect a plant's physiological status. *Proc Natl Acad Sci USA* **105**: 12081–12086

Bidadi H, Matsuoka K, Sage-Ono K, Fukushima J, Pitaksaringkarn W, Asahina M, Yamaguchi S, Sawa S, Fukuda H, Matsubayashi Y, Ono M, Satoh S (2014) CLE6 expression recovers gibberellin deficiency to promote shoot growth in *Arabidopsis*. *Plant J (in press)*

Bidadi H, Yamaguchi S, Asahina M, Satoh S (2010) Effects of shoot-applied gibberellin/gibberellin-biosynthesis inhibitors on root growth and expression of gibberellin biosynthesis genes in *Arabidopsis thaliana*. *Plant Root* **4**: 4–11

Chen WW, Yang JL, Qin C, Jin CW, Mo JH, Ye T, Zheng SJ (2010) Nitric oxide acts downstream of auxin to trigger root ferric-chelate reductase activity in response to iron deficiency in *Arabidopsis*. *Plant Physiol* **154**: 810–819

Cheng L, Wang F, Shou H, Huang F, Zheng L, He F, Li J, Zhao F-J, Ueno D, Ma JF, et al (2007) Mutation in nicotianamine aminotransferase stimulated the Fe(II) acquisition system and led to iron accumulation in rice. *Plant Physiol* **145**: 1647–1657

Cikos S, Bukovská A, Koppel J (2007) Relative quantification of mRNA: comparison of methods currently used for real-time PCR data analysis. *BMC Mol Biol* **8**: 113

- Clough SJ, Bent a F** (1998) Floral dip: a simplified method for *Agrobacterium*-mediated transformation of *Arabidopsis thaliana*. *Plant J* **16**: 735–743
- Colangelo EP, Guerinot M Lou** (2004) The essential basic helix-loop-helix protein FIT1 Is required for the iron deficiency response. *Plant Cell* **16**: 3400–3412
- Coles JP, Phillips a L, Croker SJ, García-Lepe R, Lewis MJ, Hedden P** (1999) Modification of gibberellin production and plant development in *Arabidopsis* by sense and antisense expression of gibberellin 20-oxidase genes. *Plant J* **17**: 547–556
- Connolly E, Campbell N, Grotz N** (2003) Overexpression of the FRO2 ferric chelate reductase confers tolerance to growth on low iron and uncovers posttranscriptional control. *Plant Physiol* **133**: 1102–1110
- Consequences B, Free OF, Bases RDNA** (2002) Biological consequences of freeradical-damagedDNAbases. *Free Radic Bio Med* **33**: 1–14
- Curie C, Panaviene Z, Loulergue C, Dellaporta SL, Briat JF, Walker EL** (2001) Maize yellow stripe1 encodes a membrane protein directly involved in Fe(III) uptake. *Nature* **409**: 346–349
- Curtis IS, Hanada A, Yamaguchi S, Kamiya Y** (2005) Modification of plant architecture through the expression of GA 2-oxidase under the control of an estrogen inducible promoter in *Arabidopsis thaliana* L. *Planta* **222**: 957–967

D. Abramoff M, J. Magelhaes P, J. Ram S (2004) Image processing with ImageJ. *Biophot Int* **11**: 36–42

Delhaize E (1996) A metal-accumulator mutant of *Arabidopsis thaliana*. *Plant Physiol* **111**: 849–855

Dellagi A, Segond D, Rigault M, Fagard M, Simon C, Saindrenan P, Expert D (2009) Microbial siderophores exert a subtle role in *Arabidopsis* during infection by manipulating the immune response and the iron status. *Plant Physiol* **150**: 1687–1696

Durrett TP, Gassmann W, Rogers EE (2007) The FRD3-mediated efflux of citrate into the root vasculature is necessary for efficient iron translocation. *Plant Physiol* **144**: 197–205

Enomoto Y, Hodoshima H, Shimada H, Shoji K, Yoshihara T, Goto F (2007) Long-distance signals positively regulate the expression of iron uptake genes in tobacco roots. *Planta* **227**: 81–89

Eriksson S, Böhlenius H, Moritz T, Nilsson O (2006) GA4 is the active gibberellin in the regulation of LEAFY transcription and *Arabidopsis* floral initiation. *Plant Cell* **18**: 2172–2181

Fenton H (1894) LXXIII.—Oxidation of tartaric acid in presence of iron. *J Chem Soc Trans* **65**: 899–910

García MJ, Romera FJ, Stacey MG, Stacey G, Villar E, Alcántara E, Pérez-Vicente R (2012) Shoot to root communication is necessary to control the expression of iron-acquisition genes in Strategy I plants. *Planta*.

Guerinot ML, Yi Y (1994) Iron: nutritious, noxious, and not readily available. *Plant Physiol* **104**: 815–820

- Henriques R, Jásik J, Klein M, Martinoia E, Feller U, Schell J, Pais MS, Koncz C** (2002) Knock-out of Arabidopsis metal transporter gene IRT1 results in iron deficiency accompanied by cell differentiation defects. *Plant Mol Biol* **50**: 587–97
- Hong S, Kim S a, Guerinot M Lou, McClung CR** (2013) Reciprocal interaction of the circadian clock with the iron homeostasis network in Arabidopsis. *Plant Physiol* **161**: 893–903
- Hooley R** (1994) Gibberellins: perception, transduction and responses. *Plant Mol Biol* 1529–1555
- Huang S, Raman a S, Ream JE, Fujiwara H, Cerny RE, Brown SM** (1998) Overexpression of 20-oxidase confers a gibberellin-overproduction phenotype in Arabidopsis. *Plant Physiol* **118**: 773–781
- Jiang C, Gao X, Liao L, Harberd NP, Fu X** (2007) Phosphate starvation root architecture and anthocyanin accumulation responses are modulated by the gibberellin-DELLA signaling pathway in Arabidopsis. *Plant Physiol* **145**: 1460–1470
- Jiang X, Li H, Wang T, Peng C, Wang H, Wu H, Wang X** (2012) Gibberellin indirectly promotes chloroplast biogenesis as a means to maintain the chloroplast population of expanded cells. *Plant J* 1–13
- Jin J, Hewezi T, Baum TJ** (2011) The Arabidopsis bHLH25 and bHLH27 transcription factors contribute to susceptibility to the cyst nematode *Heterodera schachtii*. *Plant J* **65**: 319–328

- Kannan S, Mathew T** (1970) Effects of growth substances on the absorption and transport of iron plants. *Plant Physiol* **45**: 206–209
- Kong WW, Yang ZM** (2010) Identification of iron-deficiency responsive microRNA genes and *cis*-elements in Arabidopsis. *Plant Physiol Bioch* **48**: 153–9
- Landsberg EC** (1981) Organic acid synthesis and release of hydrogen ions in response to Fe deficiency stress of mono- and dicotyledonous plant species. *J Plant Nutr* **3**: 579–591
- Liang G, Yang F, Yu D** (2010) MicroRNA395 mediates regulation of sulfate accumulation and allocation in Arabidopsis thaliana. *Plant J* **62**: 1046–57
- Lingam S, Mohrbacher J, Brumbarova T, Potuschak T, Fink-Straube C, Blondet E, Genschik P, Bauer P** (2011) Interaction between the bHLH transcription factor FIT and ETHYLENE INSENSITIVE3/ETHYLENE INSENSITIVE3-LIKE1 reveals molecular linkage between the regulation of iron acquisition and ethylene signaling in Arabidopsis. *Plant Cell* **23**: 1815–1829
- Liu Q, Zhang Y-C, Wang C-Y, Luo Y-C, Huang Q-J, Chen S-Y, Zhou H, Qu L-H, Chen Y-Q** (2009) Expression analysis of phytohormone-regulated microRNAs in rice, implying their regulation roles in plant hormone signaling. *FEBS Lett* **583**: 723–728
- Livak KJ, Schmittgen TD** (2001) Analysis of relative gene expression data using real-time quantitative PCR and the $2(-\Delta\Delta C(T))$ Method. *Methods* **25**: 402–408

Lucena C, Waters BM, Romera FJ, García MJ, Morales M, Alcántara E, Pérez-Vicente R (2006)

Ethylene could influence ferric reductase, iron transporter, and H⁺-ATPase gene expression by affecting FER (or FER-like) gene activity. *J Exp Bot* **57**: 4145–4154

Ma JF, Nonnato K (1996) Effective regulation of iron acquisition in graminaceous plants. The role of

mugineic acids as phytosiderophores. *Physiol Plant* **97**: 609–617

Maurer F, Müller S, Bauer P (2011) Suppression of Fe deficiency gene expression by jasmonate. *Plant*

Physiol Bioch **49**: 530–536

Mitchum MG, Yamaguchi S, Hanada A, Kuwahara A, Yoshioka Y, Kato T, Tabata S, Kamiya Y,

Sun T-P (2006) Distinct and overlapping roles of two gibberellin 3-oxidases in Arabidopsis development. *Plant J* **45**: 804–818

Murashige T, Skoog F (1962) A revised medium for rapid growth and bio assays with tobacco tissue

cultures. *Physiol Plant* **15**: 473–497

Nozoye T, Nagasaka S, Kobayashi T, Takahashi M, Sato Y, Sato Y, Uozumi N, Nakanishi H,

Nishizawa NK (2011) Phytosiderophore efflux transporters are crucial for iron acquisition in graminaceous plants. *J Biol Chem* **286**: 5446–5454

Oda A, Sakuta C, Masuda S (2003) Possible involvement of leaf gibberellins in the clock-controlled

expression of XSP30, a gene encoding a xylem sap lectin, in cucumber roots. *Plant Physiol* **133**: 1779–1790

- Olszewski N, Sun T, Gubler F** (2002) Gibberellin signaling biosynthesis, catabolism, and response pathways. *Plant Cell* **14**: S61–S81
- Pan RC, Zheng SCS, Mo SG** (1991) Influence of paclobutrazol on mineral element content of rice seedlings. *J Plant Nutr* **14**: 1–6
- Pant BD, Buhtz A, Kehr J, Scheible W-R** (2008) MicroRNA399 is a long-distance signal for the regulation of plant phosphate homeostasis. *Plant J* **53**: 731–738
- Pe R, García MJ, Lucena C, Romera FJ, Alcántara E, Pérez-Vicente R** (2010) Ethylene and nitric oxide involvement in the up-regulation of key genes related to iron acquisition and homeostasis in *Arabidopsis*. *J Exp Bot* **61**: 3885–3899
- Peng J, Harberd NP** (1997) Gibberellin deficiency and response mutations suppress the stem elongation phenotype of phytochrome-deficient mutants of *Arabidopsis*. *Plant Physiol* **113**: 1051–1058
- Plackett ARG, Powers SJ, Fernandez-Garcia N** (2012) Analysis of the developmental roles of the *Arabidopsis* gibberellin 20-oxidases demonstrates that GA20ox1, -2, and -3 are the dominant paralogs. *Plant Cell* **24**: 941–960
- Proebsting WM, Hedden P, Lewis MJ, Croker SJ, Proebsting LN** (1992) Gibberellin concentration and transport in genetic lines of pea: effects of grafting. *Plant Physiol* **100**: 1354–1360

Ragni L, Nieminen K, Pacheco-Villalobos D, Sibout R, Schwechheimer C, Hardtke CS (2011)

Mobile gibberellin directly stimulates Arabidopsis hypocotyl xylem expansion. *Plant Cell* **23**: 1322–1336

Rieu I, Eriksson S, Powers SJ, Gong F, Griffiths J, Woolley L, Benlloch R, Nilsson O, Thomas SG,

Hedden P, et al (2008a) Genetic analysis reveals that C19-GA 2-oxidation is a major gibberellin inactivation pathway in Arabidopsis. *Plant Cell* **20**: 2420–2436

Rieu I, Ruiz-Rivero O, Fernandez-Garcia N, Griffiths J, Powers SJ, Gong F, Linhartova T,

Eriksson S, Nilsson O, Thomas SG, et al (2008b) The gibberellin biosynthetic genes AtGA20ox1 and AtGA20ox2 act, partially redundantly, to promote growth and development throughout the Arabidopsis life cycle. *Plant J* **53**: 488–504

Robinson NJ, Procter CM, Connolly EL, Guerinot ML (1999) A ferric-chelate reductase for iron

uptake from soils. *Nature* **397**: 694–697

Romfield V, Marschner H (1981) Iron deficiency stress induced morphological and physiological

changes in root tips of sunflower. *Physiol Plant* **53**: 354–360

Sankhla N, Davis TD, Jolley VD, Upadhyaya A (1986) Effect of paclobutrazol on the development of

iron chlorosis in soybeans. *J Plant Nutr* **9**: 923–934

Séguéla M, Briat J-F, Vert G, Curie C (2008) Cytokinins negatively regulate the root iron uptake

machinery in Arabidopsis through a growth-dependent pathway. *Plant J* **55**: 289–300

- Sekimoto H, Kato A, Nomura T** (2002) Chlorosis induced by iron deficiency is more severe in gibberellin-deficient dwarf plants. *Plant Nutr* **92**: 150–151
- Sekimoto H, Matsuura K, Yoshino T** (1998) Relationship between the greening of leaves by the treatment with a gibberellin-biosynthesis inhibitor and leaf area or nitrogen content in *Cucumis sativus* L. *Plant Physiol Bioch* **67**: 270–272
- Sivitz A, Grinvalds C, Barberon M, Curie C, Vert G** (2011) Proteasome-mediated turnover of the transcriptional activator FIT is required for plant iron-deficiency responses. *Plant J* **66**: 1044–1052
- Stoltzfus RJ** (2001) Defining iron-deficiency anemia in public health terms: a time for reflection. *ASNS* **131**: 565S–567S
- Tanimoto E** (1987) Gibberellin-dependent root elongation in *Lactuca sativa*: recovery from growth retardant-suppressed elongation with thickening by low concentration of GA3. *Plant Cell Physiol* **28**: 963–973
- Thorstensen T, Grini PE, Mercy IS, Alm V, Erdal S, Aasland R, Aalen RB** (2008) The Arabidopsis SET-domain protein ASHR3 is involved in stamen development and interacts with the bHLH transcription factor ABORTED MICROSPORES (AMS). *Plant Mol Biol* **66**: 47–59
- Tottey S, Block M a, Allen M, Westergren T, Albrieux C, Scheller H V, Merchant S, Jensen PE** (2003) Arabidopsis CHL27, located in both envelope and thylakoid membranes, is required for the synthesis of protochlorophyllide. *Proc Natl Acad Sci USA* **100**: 16119–16124

- Vert GA, Briat J-F, Curie C** (2003) Dual regulation of the Arabidopsis high-affinity root iron uptake system by local and long-distance signals. *Plant Physiol* **132**: 796–804
- Vigani G, Morandini P, Murgia I** (2013) Searching iron sensors in plants by exploring the link among 2'-OG-dependent dioxygenases, the iron deficiency response and metabolic adjustments occurring under iron deficiency. *Front Plant Sci* **4**: 169
- Wang B, Li Y, Zhang W-H** (2012) Brassinosteroids are involved in response of cucumber (*Cucumis sativus*) to iron deficiency. *Ann Bot* **110**: 681–688
- Wang H-Y, Klatte M, Jakoby M, Bäumlein H, Weisshaar B, Bauer P** (2007) Iron deficiency-mediated stress regulation of four subgroup Ib BHLH genes in *Arabidopsis thaliana*. *Planta* **226**: 897–908
- Wang N, Cui Y, Liu Y, Fan H, Du J, Huang Z, Yuan Y, Wu H, Ling H-Q** (2013) Requirement and Functional Redundancy of Ib Subgroup bHLH Proteins for Iron Deficiency Responses and Uptake in *Arabidopsis thaliana*. *Mol Plant* **6**: 503–13
- Willige BC, Isono E, Richter R, Zourelidou M, Schwechheimer C** (2011) Gibberellin regulates PIN-FORMED abundance and is required for auxin transport-dependent growth and development in *Arabidopsis thaliana*. *Plant Cell* **23**: 2184–95
- Willige BC, Ogiso-Tanaka E, Zourelidou M, Schwechheimer C** (2012) WAG2 represses apical hook opening downstream from gibberellin and PHYTOCHROME INTERACTING FACTOR 5. *Development* **139**: 4020–8

Von Wiren N, Mori S, Marschner H, Romheld V (1994) Iron inefficiency in maize mutant *ysl* (*Zea mays* L. cv Yellow-Stripe) is caused by a defect in uptake of iron phytosiderophores. *Plant Physiol* **106**: 71–77

Yamaguchi S, Smith MW, Brown RG, Kamiya Y, Sun T (1998) Phytochrome regulation and differential expression of gibberellin 3 β -hydroxylase genes in germinating *Arabidopsis* seeds. *Plant Cell* **10**: 2115–2126

Yuan Y, Wu H, Wang N, Li J, Zhao W, Du J, Wang D, Ling H-Q (2008) FIT interacts with AtbHLH38 and AtbHLH39 in regulating iron uptake gene expression for iron homeostasis in *Arabidopsis*. *Cell Res* **18**: 385–397

Table and Figures

Table 1. List of the gene specific primer

For real time PCR			
AGI number	Description	Sequence	PCR product size (bp)
AT4G19690	IRT1	F 5'-AAGCTTTGATCACGGTTGG-3' R 5'-TTAGGTCCCATGAACTCCG-3'	100
AT1G01580	FRO2	F 5'-CTTGGTCATCTCCGTGAGC-3' R 5'-AAGATGTTGGAGATGGACGG-3'	122
AT2G28160	FIT	F 5'-CCCCTGTTTCATAGACGAGAAC-3' R 5'-CTCTAACACTATCACCGTCGAAG-3'	125
AT3G56970	bHLH038	F 5'-CGGTCGCGAGTTATCTCTCAAC-3' R 5'-CCCACCCAACACATTTGATATCG-3'	116
AT3G56980	bHLH039	F 5'-GACGGTTTCTCGAAGCTTG-3' R 5'-GGTGGCTGCTTAACGTAACAT-3'	132
At4g25420	GA20ox1	F 5'-CGAGAGCGAGAGGAAATCAC-3' R 5'-GTGAAGTCAGGGTATCTTCTTGATG-3'	114
At5g51810	GA20ox2	F 5'-CCAATCCAAGGCTTTCGTTG-3' R 5'-CGCGCTCTCTCTATTCACAAC-3'	107
AT5G07200	GA20ox3	F 5'-GTGAACAGCGAGAGAGAAAGGAAG-3' R 5'-CACCAGACTTCACTCCGTTTACTAG-3'	106
At1g15550	GA3ox1	F 5'-CCCGGTTATCTGTAGCATTCC-3' R 5'-TTCCATGTCACCGATTGGTATAG-3'	112
At1g80340	GA3ox2	F 5'-CCGATATAATGATCTCTCCACTTC-3' R 5'-AGCTTTGGTAGCAAGGTATTG-3'	98
AT1G78440	GA2ox1	F 5'-CTTCGCTGGACCTTCATTGAC-3' R 5'-GACCAAGTAAACTCCTCGTACAAC-3'	93
At1g80340	GA2ox2	F 5'-GGAGGAAGAGGCGGAGAAGATG-3' R 5'-GAAGACCCGCCGTGTTATTAG-3'	98
AT5G09810	ACT7	F 5'-CAGTGTCTGGATCGGAGGAT-3' R 5'-TGAACAATCGATGGACCTGA-3'	102
For RT PCR			
AGI number	Description	Sequence	PCR product size (bp)
AT2G28160	FIT	F 5'-CGTAGCTTCGACGGTGATAG-3' R 5'-TCCGGAGAAGGAGAGCTTAG-3'	566
AT5G09810	ACT7	F 5'-CAATGTCCCTGCCATGTATG-3' R 5'-TGAACAATCGATGGACCTGA-3'	732
For Genotyping			
	primer	Sequence	
	fit-2 -F	5'-CTTGGTCCATTACAAAACAGC-3'	
	fit-2 -R	5'-TTGACTCACGTTAGAGCAAGC-3'	
	Lb1.3	5'-ATTTTGCCGATTTCCGGAAC-3'	

Figure 1. GA₄ application on shoots promoted shoot growth and expression of Fe-uptake-related genes in roots. (A) Effect of shoot-applied GA₄ in *ga3ox1 ga3ox2*. Three-week-old seedlings grown on MS medium were treated with 0, 0.01, 0.1, 1, or 10 μM GA₄ applied onto the shoot for 3 days. Bars = 5 mm. (B) Relative shoot fresh weight of plants shown in A, obtained by comparison with plants grown with 0 μM GA₄. Data are means ± SD (*n* = 14). (C) Expression levels of *IRT1* and *FRO2* were determined using quantitative RT-PCR, relative to 0 μM GA₄. Data are means of triplicate experiments ± SD. Total RNA was prepared from roots. *ACT7* was amplified for an internal control. Asterisks and double asterisks indicate statistical differences by Dunnett's test (**P* < 0.05, ***P* < 0.01) compared with 0 μM GA₄.

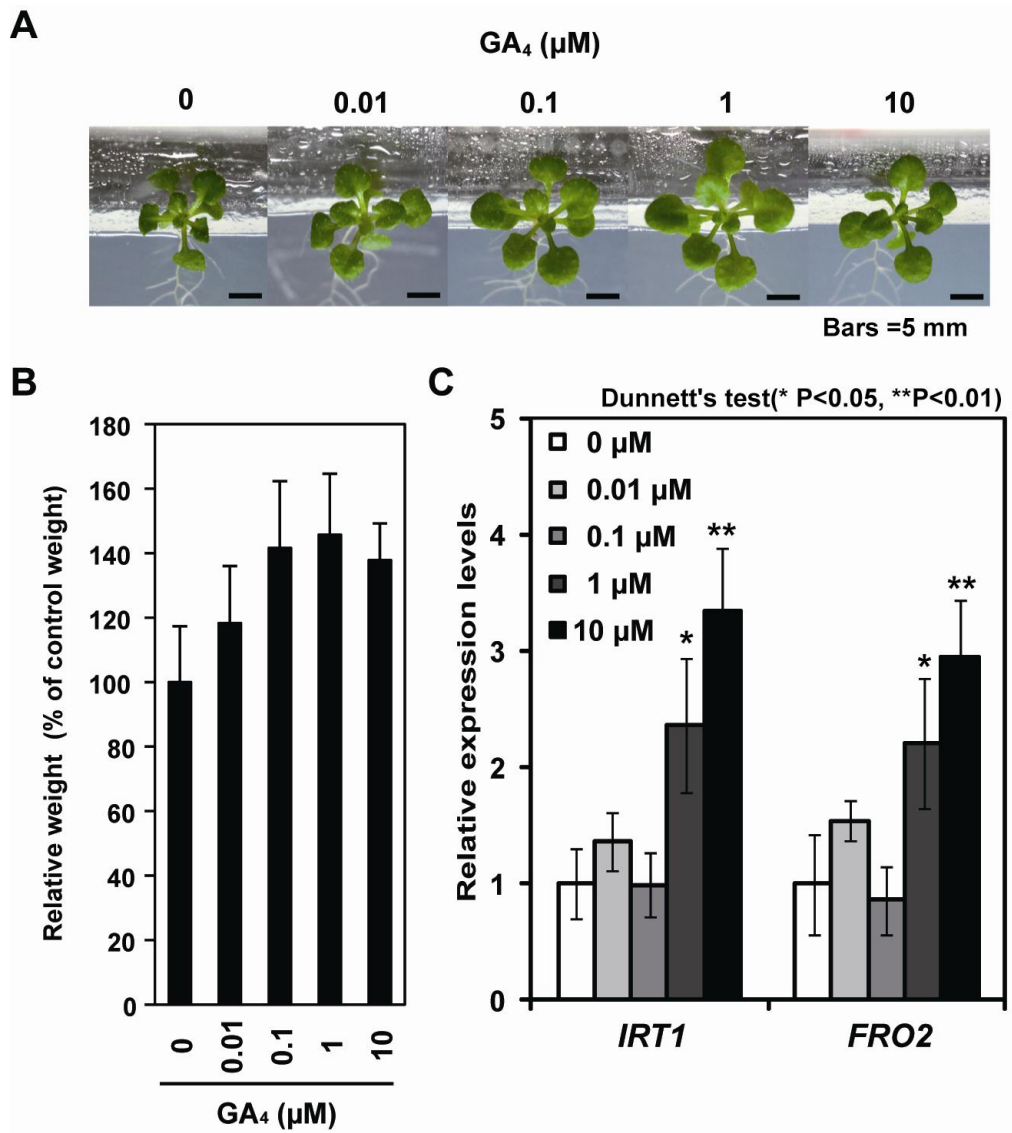


Figure 2. Comparison of Fe contents in WT and *ga3ox1 ga3ox2* with (GA) or without (mock) shoot-applied GA₄. WT and *ga3ox1 ga3ox2* were grown in MS medium containing 50 μM Fe. Every 5 days, 10 μM GA₄ or mock solution (distilled water) was applied onto the shoots. The Fe contents in shoots and roots of 20-day-old seedlings were separately determined by ICP-OES. Data are means ± SD (*n* = 3). Different letters indicate statistical differences according to the Tukey test (*P* < 0.05). (A, B) Fe concentrations on a dry-weight basis (A, C) and total content (B, D) in roots (A, B) or shoots (C, D).

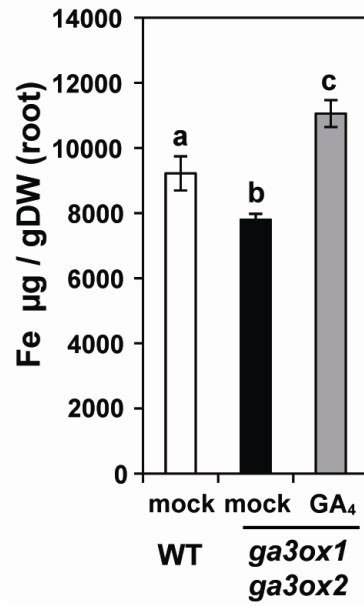
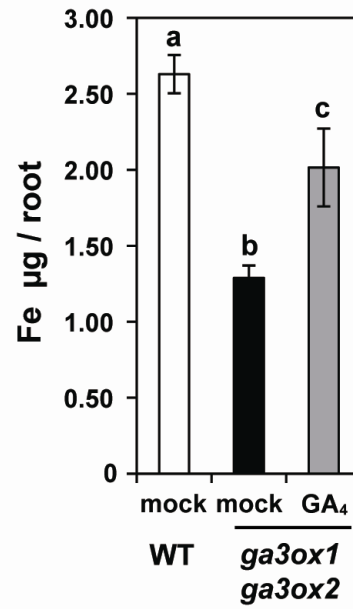
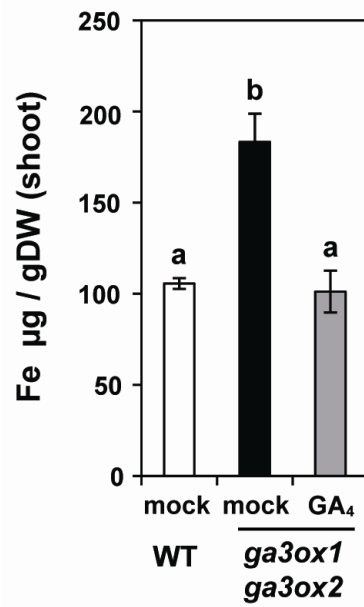
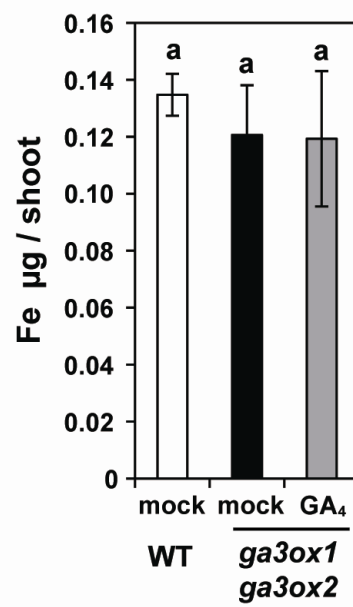
A**B****C****D**

Figure 3. GA₄ treatment of roots slightly enhanced the expression of Fe-uptake-related genes in roots. (A) Effect of root-applied GA₄ in *ga3ox1 ga3ox2*. Three-week-old seedlings were grown for 3 days on MS medium containing 0, 0.001, 0.01, 0.1, or 1 μM GA₄. Bars = 5 mm. (B) Percentages of shoot fresh weight relative to plants grown with 0 M GA₄. Data are means ± SD (*n* = 14). (C) Levels of *IRT1* and *FRO2* expression determined using quantitative RT-PCR, relative to 0 μM GA₄. Data are means of triplicate experiments ± SD. Total RNA was prepared from roots. Asterisks and double asterisks indicate statistical differences according to Dunnett's test (**P* < 0.05, ***P* < 0.01) compared with 0 μM GA₄.

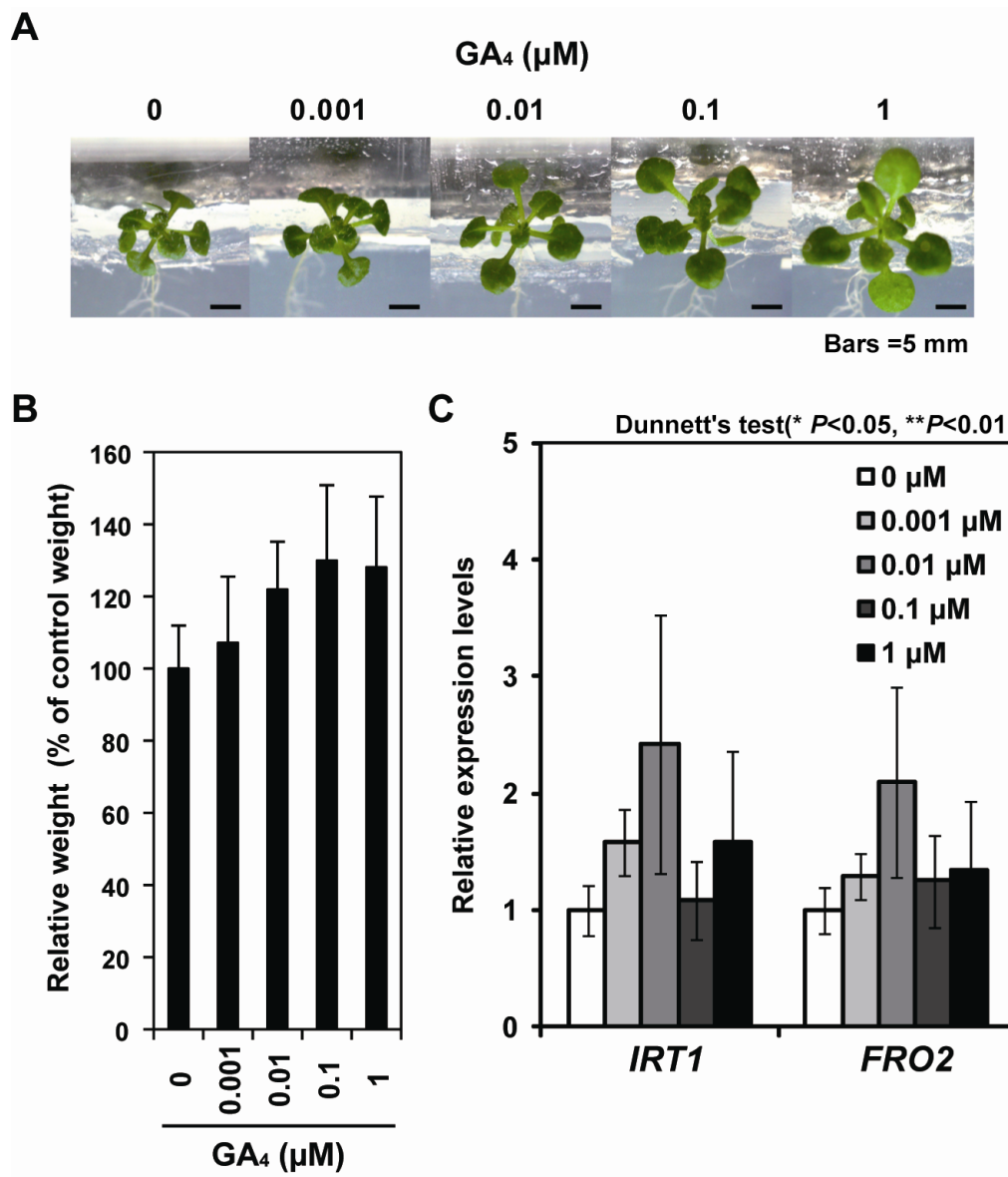


Figure 4. Comparison of the WT and *ga3ox1 ga3ox2* responses to Fe deficiency. (A) Root-hair formation under Fe-sufficient and Fe-deficient conditions. Ten-day-old WT and *ga3ox1 ga3ox2* plants were transferred to either Fe-sufficient medium (+ Fe: 100 μ M Fe-EDTA) or Fe-deficient medium (– Fe: 0 μ M Fe-EDTA with 200 μ M ferrozine) and the primary roots were observed after 4 days using light microscopy. Bars = 0.5 mm. (B) Root-hair densities of WT and *ga3ox1 ga3ox2* plants shown in A. Root-hair densities were measured on three 1-mm segments from the root tip. Bars show the means \pm SD ($n > 20$). Groups with different letters were statistically different ($P < 0.05$, Steel-Dwass test).

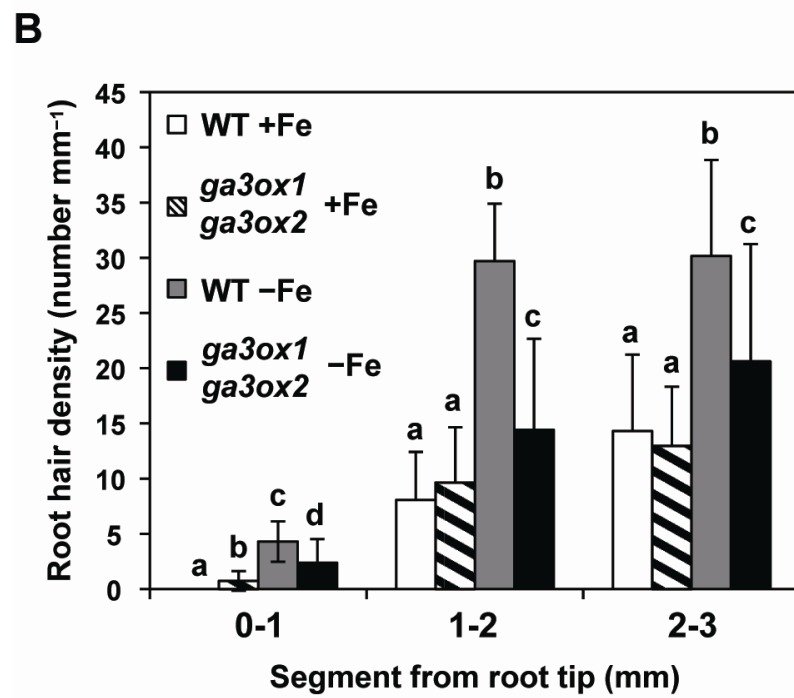
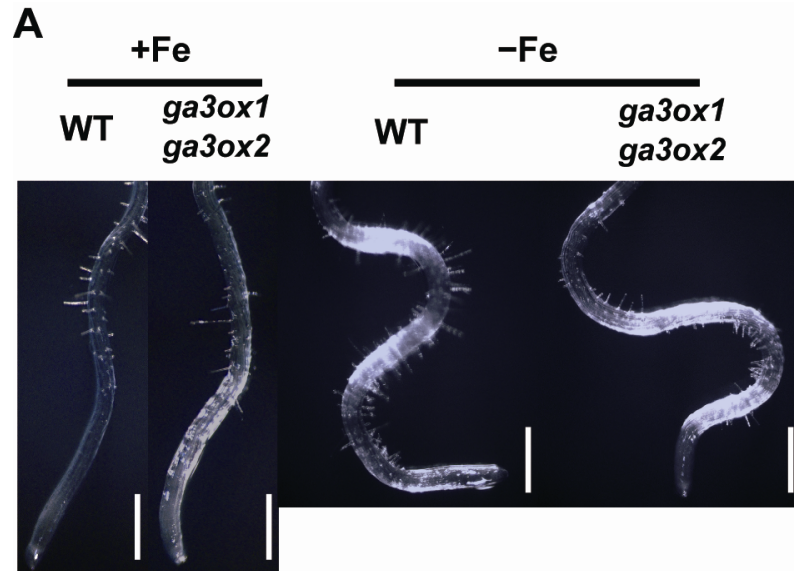


Figure 5. Expression of Fe-uptake-related genes in WT and *ga3ox1 ga3ox2* plants grown under Fe-sufficient and Fe-deficient conditions. (A) Three-week-old WT and *ga3ox1 ga3ox2* plants were grown as described in Fig. 4 for 3 days and total RNA was prepared from the roots. The levels of *IRT1* and *FRO2* transcripts were examined using quantitative RT-PCR relative to the WT grown in Fe-sufficient medium. Data are means of triplicate experiments \pm SD. Asterisks indicate statistical differences between the Fe-sufficient and Fe-deficient conditions according to the Student's t-test ($P < 0.05$). (B) Three-week-old WT and *ga3ox1 ga3ox2* were subjected to Fe-deficiency treatment and GA₄ application onto the shoot for 3 days. Mock treatments were performed using water instead of GA₄. *IRT1* expression relative to mock treatment of the WT was determined in root samples using quantitative RT-PCR. Data are means of triplicate experiments \pm SD. Different letters indicate statistical differences according to the Tukey test ($P < 0.01$). (C) The WT and *ga3ox1 ga3ox2* plants shown have a typical shoot phenotype, as indicated in (B). Bars = 10 mm.

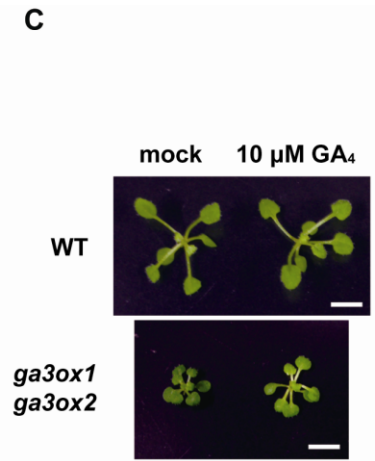
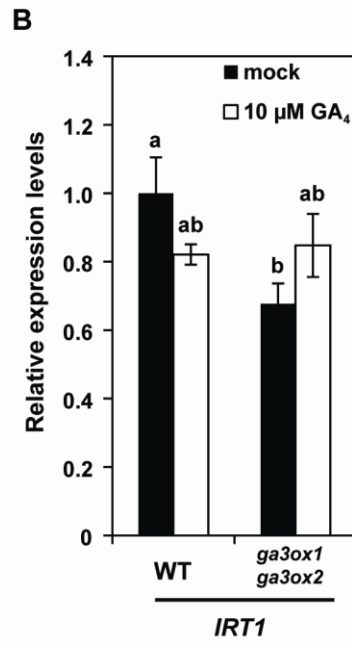
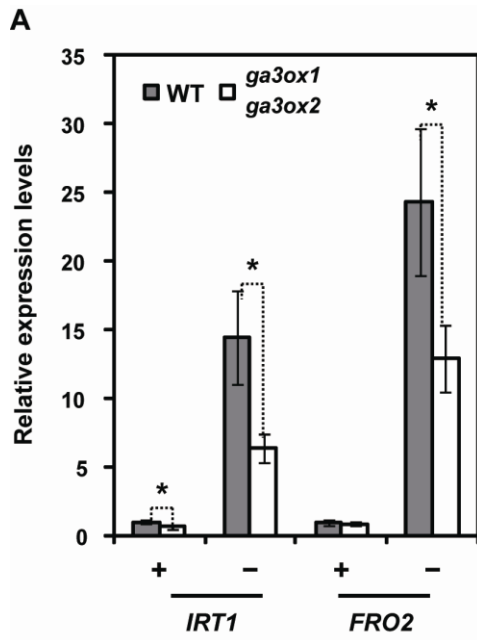


Figure 6. Effect of Fe deficiency on the expression of GA biosynthetic genes. Three-week-old WT plants were grown as described in Fig. 5. Total RNA was prepared from the shoots (A, B) and roots (C, D). Expression levels of GA biosynthetic genes (*GA3ox1*, *GA3ox2*, *GA20ox1*, *GA20ox2*, and *GA20ox3*) and GA catabolic genes (*GA2ox1* and *GA2ox2*) were examined using quantitative RT-PCR relative to the *ACT7* level. Inset shows a magnified graph of the *GA20ox3* expression level. Data are means of triplicate experiments \pm SD. Asterisks indicate statistical differences according to the Student's t-test ($P < 0.05$).

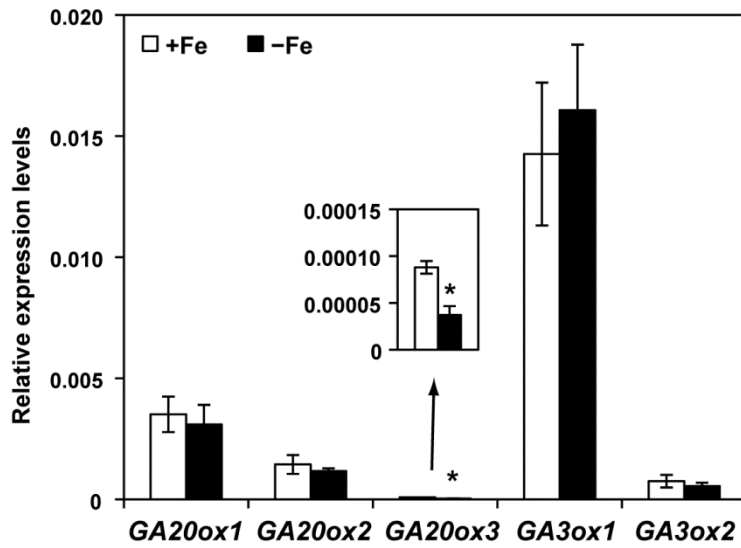
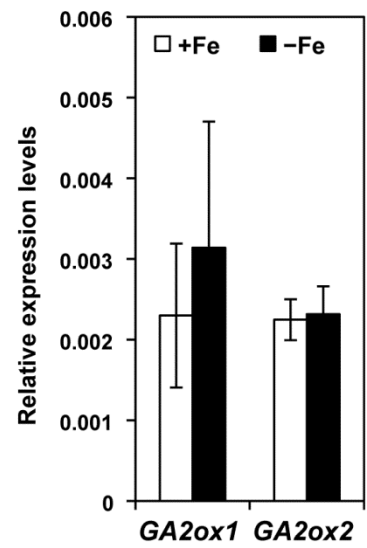
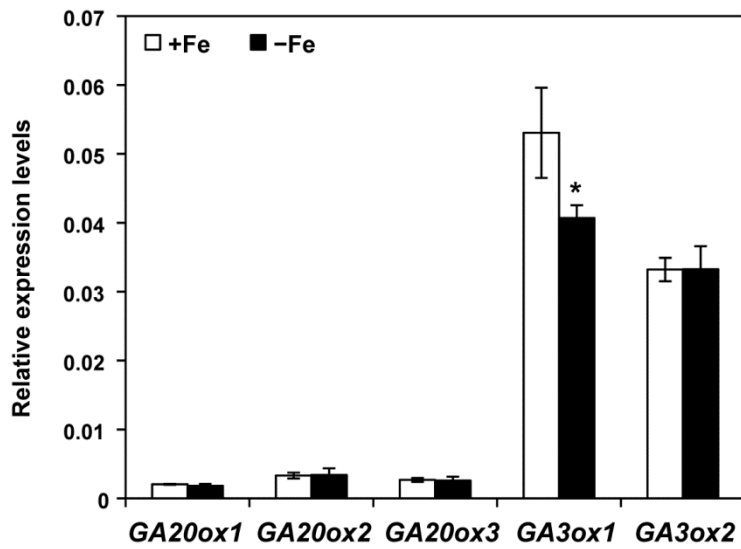
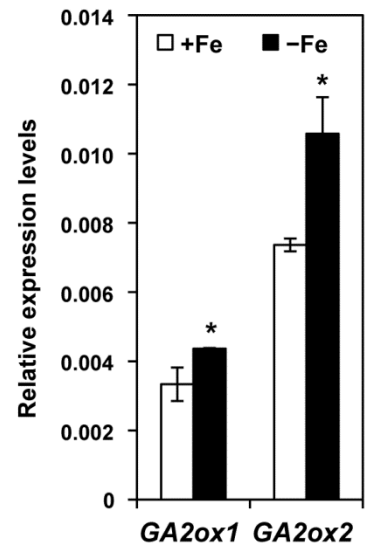
A**B****C****D**

Figure 7. Effect of GA₄ application on the expression of bHLH-type TF genes. GA₄ applications to shoot (A) and root (B) were performed as described in Fig. 1 and 3, respectively. Expression levels of *FIT*, *bHLH038* and *bHLH039* were determined using quantitative RT-PCR, relative to 0 μM GA₄. Data are means of triplicate experiments ± SD. Total RNA was prepared from roots. *ACT7* was amplified for an internal control. Asterisks and double asterisks indicate statistical differences by Dunnett's test (**P* < 0.05, ***P* < 0.01) compared with 0 μM GA₄.

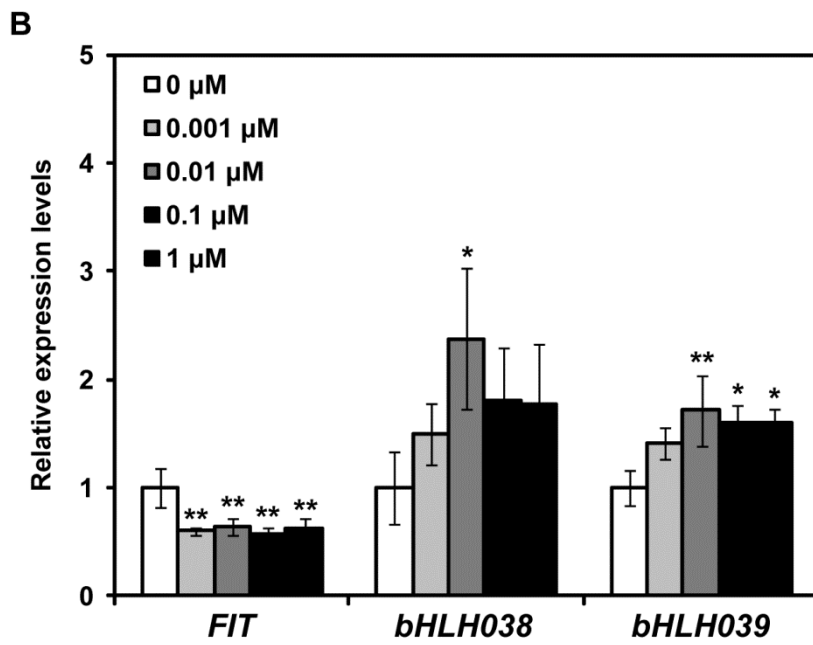
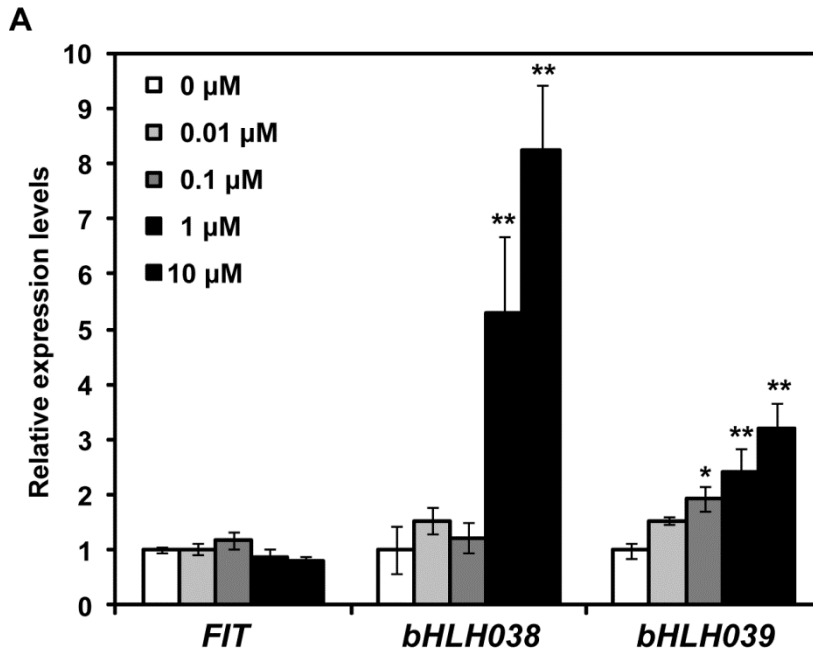


Figure 8. Time course of the expression of Fe-uptake-related genes, such as *IRT1*, *bHLH038* and *FIT*, after GA₄ application in *ga3ox1 ga3ox2*. Roots samples were harvested at 0, 6, 12, 24, 48 and 72 hours after 10 μM GA₄ application on 3-week-old *ga3ox1 ga3ox2* shoot. Expression levels of *IRT1*, *FIT* and *bHLH038* were determined using quantitative RT-PCR, relative to 0 hours. Data are means of triplicate experiments ± SD. Asterisks and double asterisks indicate statistical differences by Dunnett's test (**P* < 0.05, ***P* < 0.01) compared with 0 hours.

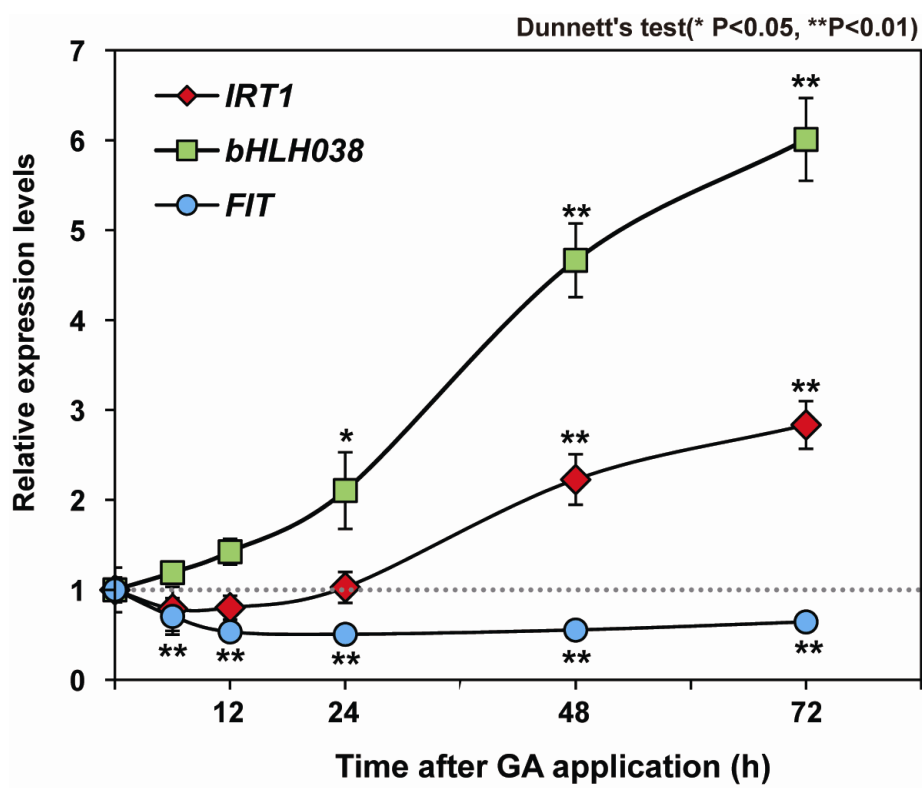


Figure 9. Effect of GA₄ on the expression of bHLH transcription factors in shoots. (A) Three-week-old *ga3ox1 ga3ox2* plants were treated with 0 or 10 μM GA₄ applied onto the shoot for 3 days. Using quantitative RT-PCR with shoot samples, *bHLH038* and *bHLH039* expression was compared in plants treated with GA₄ or mock treated only. Data are means of triplicate experiments ± SD. (B) The histochemical assay in *ga3ox1 ga3ox2* transformed with GUS gene driven by *bHLH038* promoter. Seedlings after 3 days with 0 or 10 μM GA₄ application to shoot. Bars = 10 mm.

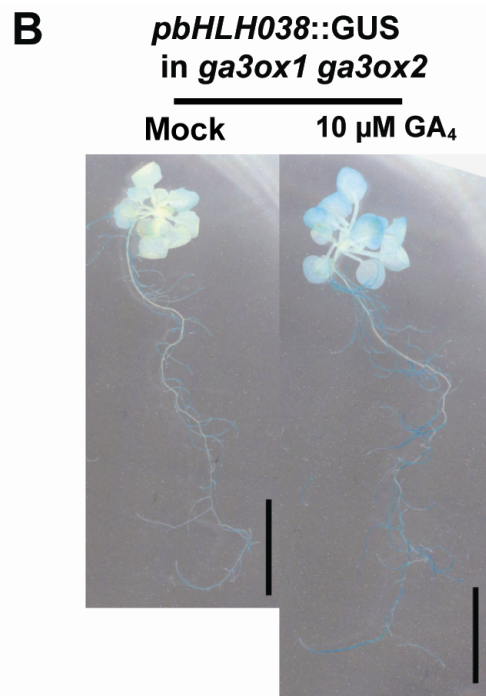
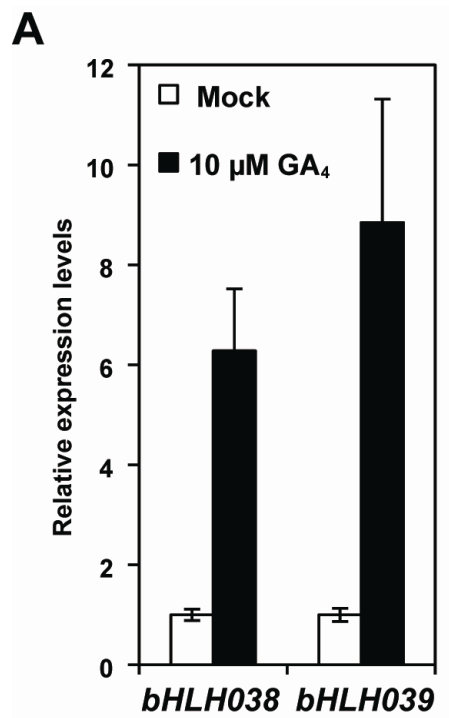


Figure 10. Expression of bHLH-type TF genes in WT and *ga3ox1 ga3ox2* plants grown under Fe-sufficient and Fe-deficient conditions. Total RNA was prepared from the shoots (A) and roots (B). Expression levels of *FIT*, *bHLH038* and *bHLH039* were determined as described in Fig. 5.

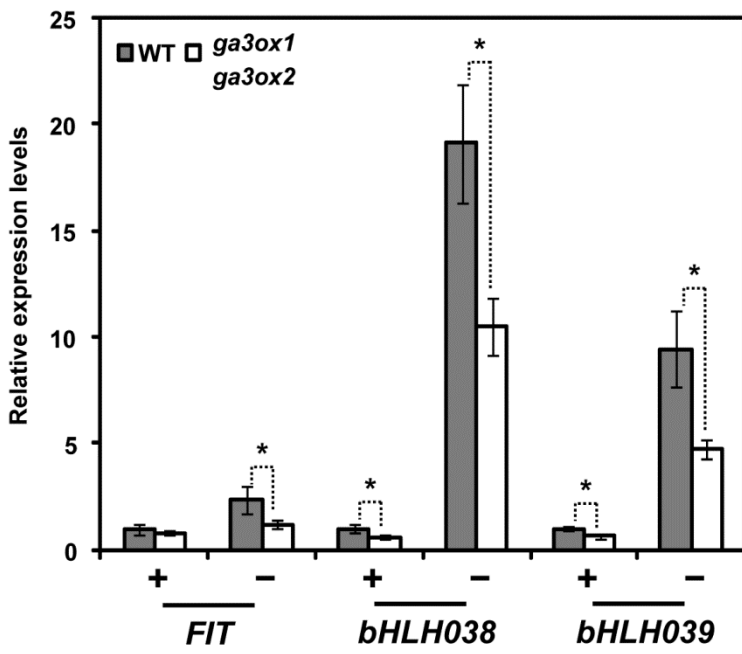
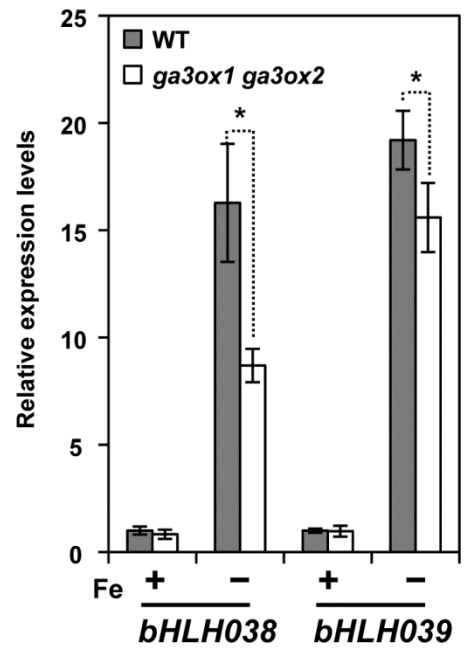
A**B**

Figure 11. Effect of shoot-applied GA₄ on the expression of Fe-uptake-related genes in WT and the *fit-2* mutant supplied with a GA biosynthesis inhibitor. (A) At 5 days after sowing, WT and *fit-2* were transferred to MS medium supplied with 1 μM PBZ. Three-week-old seedlings with (+) or without (-) shoot-applied 10 μM GA₄ for 3 days were harvested. Quantitative RT-PCR was performed using total RNA prepared from roots. Data are means of triplicate experiments ± SD. Asterisks indicate statistical differences according to the Student's t-test ($P < 0.05$) between mock and GA₄-treated samples. The inset graph shows magnifications of the regions of the graph indicated by arrows. (B) Absence of full-length *FIT* transcript in the *fit-2* mutant. *FIT* expression was determined by semi-quantitative RT-PCR in root samples of WT and *fit-2* plants on two independent replicates. *FIT* transcripts were amplified with primers designed across the T-DNA. *ACT7* was used as an internal control.

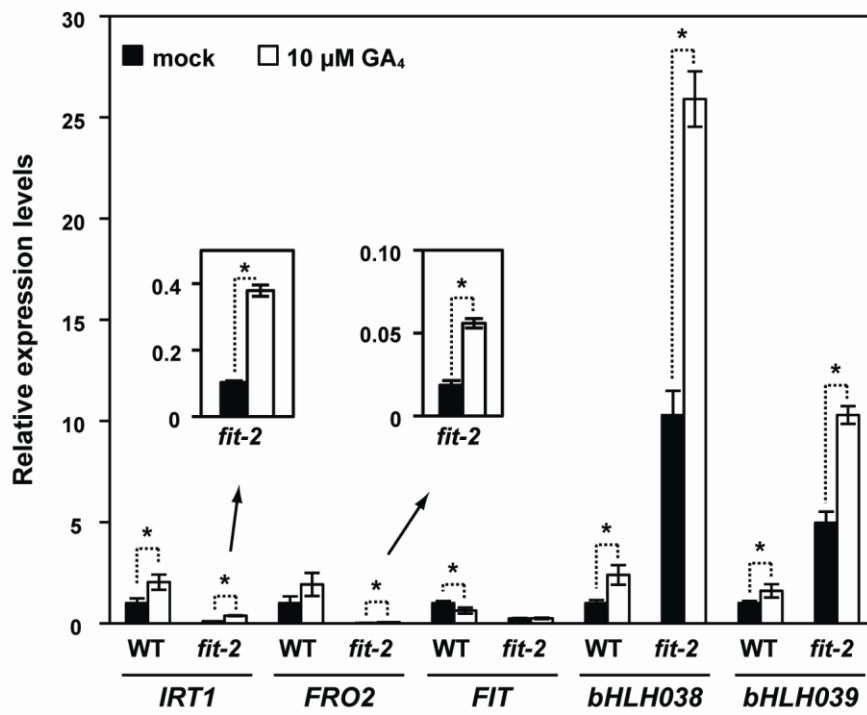
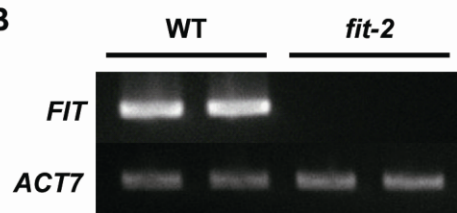
A**B**

Figure 12. Effect of PBZ on *IRT1* expression in the *fit-2* mutant under Fe deficiency. At 5 days after sowing, WT and *fit-2* plants were transferred to MS medium containing or lacking 1 μ M PBZ. Three-week-old seedlings were subjected to Fe deficiency with or without PBZ for 3 days. Real-time RT-PCR was performed using total RNA prepared from roots. Data are means of triplicate experiments \pm SD. Inset graph shows *IRT1* expression levels in *fit-2* under Fe-deficient conditions.

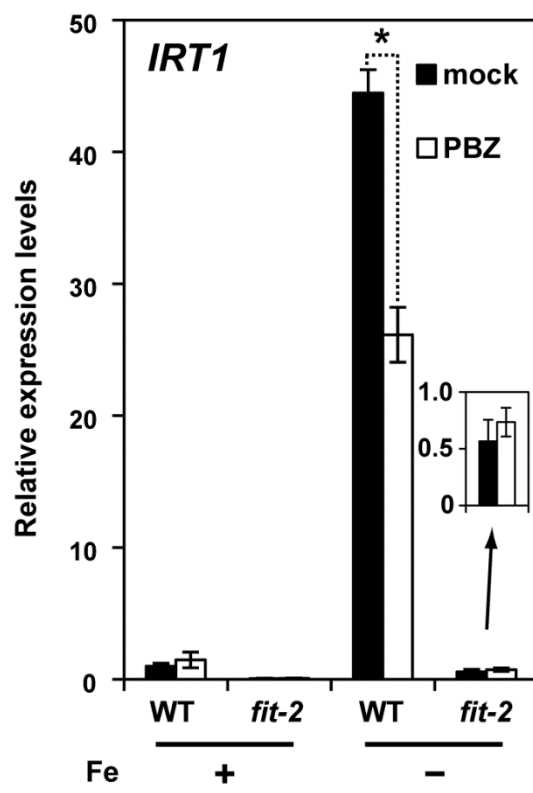
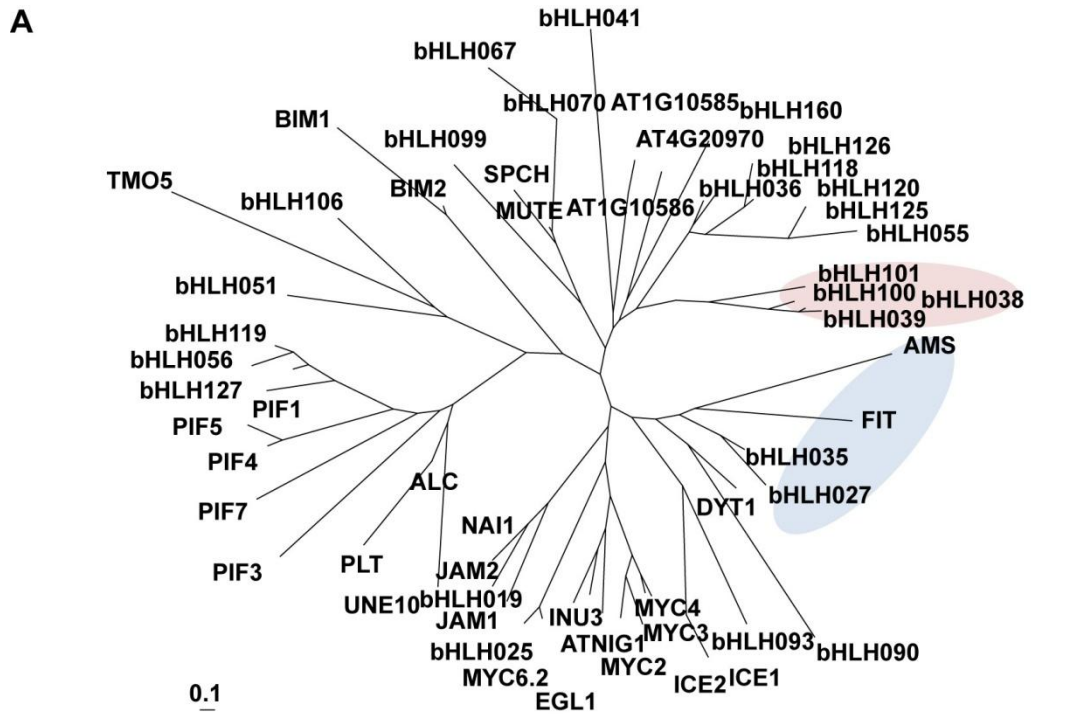


Figure 13. bHLH-type TF family in *Arabidopsis*. (A) An unrooted Neighbour-joining phylogenetic tree of bHLH038 and FIT generated from amino acid sequences of proteins by ClustalW. (B) Percentage of identities was calculated for each pairwise combination. Top four bHLH-type TFs with homology to bHLH038 and FIT indicate the red and blue color range, respectively.



B

	bHLH038	bHLH039	bHLH100	bHLH101	FIT	AMS	bHLH027	bHLH035
bHLH038								
bHLH039	79							
bHLH100	57	60						
bHLH101	32	31	29					
FIT	14	15	9	12				
AMS	16	18	19	15	22			
bHLH027	15	11	12	15	18	18		
bHLH035	14	14	13	12	20	23	50	

Acknowledgments

I wish to express my sincere appreciation to Professor S. Satoh of the University of Tsukuba for his suggestions, constructive criticisms and excellent experimental environment throughout the course of my research.

I am sincerely grateful to Assistant Professor J. Furukawa of the University of Tsukuba for continuing support and technical advice.

I am also grateful to Dr. H. Bidadi for supporting data and technical manipulation.

My special thanks are due to Dr. M. Asahina (Teikyo University), Dr. K. Miura (University of Tsukuba), Dr. H. Iwai (University of Tsukuba), Dr. T. Mizoguchi (International Christian University), Dr. H. Kamata (University of Tsukuba), M. Ono (University of Tsukuba), N. Nakajima (University of Tsukuba), M. Tamaoki (University of Tsukuba) for valuable advice.

I appreciate Dr. K. Sage-Ono (University of Tsukuba) for providing the destination vector and Dr. S. Yamaguchi (Tohoku University) for providing the *ga3ox1 ga3ox2* seed.

Many thanks are due to the members of the laboratory of Plant physiology Research group, of the University of Tsukuba, for their encouragement and useful discussion.

Last but not least, I would like to thank my parents for all their help and economical support.